

THS 224/1103

THESIS



This is to certify that the

thesis entitled

A COMPARISON OF PEAK ACCELERATION IN CUSHIONED DROPS: ACCELEROMETERS VS. HIGH-SPEED VIDEO METHOD

presented by

Jeffery S. Waldeck

has been accepted towards fulfillment of the requirements for

M.S. degree in Packaging

Major professor

Date April 28, 1989



RETURNING MATERIALS:
Place in book drop to remove this checkout from your record. FINES will be charged if book is returned after the date stamped below.

A COMPARISON OF PEAK ACCELERATION IN CUSHIONED DROPS: ACCELEROMETERS VS. HIGH-SPEED VIDEO METHOD

Ву

Jeffery S. Waldeck

A THESIS

Submitted to

Michigan State University
in partial fulfillment of the requirements
for the degree of

MASTER OF SCIENCE

School of Packaging

1989

ABSTRACT

A COMPARISON OF PEAK ACCELERATION IN CUSHIONED DROPS: ACCELEROMETERS VS. HIGH-SPEED VIDEO METHOD

By

Jeffery S. Waldeck

A quick summary is presented of some conventional methods for measuring the deceleration of a cushioned product in an impact and their limitations. A new method involving a high-speed video camera is developed. The procedure involves filming compression-expansion process of the cushion during impact and afterwards measuring displacement values over time from the video screen. By fitting a high order polynomial function to this data and then obtaining its second derivitive, the peak deceleration produced during the impact is obtained. The peak deceleration value obtained with an accelerometer is compared to that obtained using the high-speed video camera. The peak compression values of the cushions during the impact are also measured.

Copyright by

JEFFERY SCOTT WALDECK

1989

DEDICATION

I would like to dedicate this thesis to my mother, Carol Hart Melvin, in recognition of the constant support she gave me and the sacrifices she made throughout my education.

ACKNOWLEDGEMENTS

I would like to thank Dr. Gary Burgess for acting as my advisor on this study. The constant assistance and direction he provided was greatly appreciated, especially at those times when all did not proceed as planned. Above all I cherish his friendship and humor, without which I would have been hard pressed to finish this study.

I am also greatful to the other members of my committee for their assistance. To Dr. Diana Twede for her moral support and constant encouragement. To Dr. George Mase for his time and effort. And to Dr. Paul S. Singh for suggesting this topic of study.

I would also like to thank Susan and Gene McDonald for generously allowing me the use of their personal computer in typing this thesis. Their assistance and support was invaluable to me throughout the editing process.

TABLE OF CONTENTS

List of	Tables iv	•
List of	Figures v	,
List of	Symbols vi	i
Chapter	1 - INTRODUCTION 1	
Chapter	2 - A NEW METHOD 13	ı
Chapter	3 - DATA AND RESULTS	1
	4 - LIMITATIONS AND SUGGESTIONS FOR	
	FUTURE RESEARCH 48	ì
	FUTURE RESEARCH	
Chapter Appendix Appendix Appendix		}

LIST OF TABLES

		PAGE	3
Table	1	Values of inches/pixel calculated in study 29	}
Table	2	Results of both methods using 2" thick cushions 37	7
Table	3	Results of both methods using 3" thick cushions 38	3
Table	4	Percent total compression at peak cushion deformation for 2" and 3" thick cushions 46	5
Table	5	Position of platen vs. time from high-speed video method for 2" thick cushions 53	3
Table	6	Position of platen vs. time from high-speed video method for 3" thick cushions 54	4
Table	7	Data from accelerometer method for 2" thick cushions 55	5
Table	8	Data from accelerometer method for 3" thick cushions 56	5

LIST OF FIGURES

		PAC	E
Figure	1	Trade-off between package cost and damage cost	2
Figure	2	Methodology for determining cushioning needed	2
Figure	3	Typical cushion curve	4
Figure	4	Typical shock pulse recorded by an accelerometer	8
Figure	5	View screen of Kodak's Ectapro 1000 system 1	. 4
Figure	5 a	Cushion as it appears before compression	. 4
Figure	5b	Cushion as it appears during compression	. 4
Figure	6	Illustration of angular offset error l	9
Figure	6 a	High-speed video setup l	9
Figure	6b	Test platen interference 1	9
Figure	6 c	Trigonometric error analysis l	. 9
Figure	7	Test setup for the accelerometer method	22
Figure	8	Test setup for the high-speed video method	23
Figure	9	Typical displacement plot of cushion compression	27
Figure	10	Determination of P (inches/pixel) from sample	28
Figure	11	Weights and static loadings used in tests	3 3

	P.	AGE
Figure 12	Summary of test conditions	35
Figure 13	Results of both methods at a 30" drop height	39
Figure 14	Results of both methods at a 36" drop height	40
Figure 15	Results of both methods at a 42" drop height	41
Figure 16	Dow Chemical Co. data for a 30" drop height	42
Figure 17	Dow Chemical Co. data for a 36" drop height	43
Figure 18	Dow Chemical Co. data for a 42" drop height	44
Figure 19	Percent compression at peak cushion displacement	47
Figure 20	Video error analysis, maximum case	59
Figure 21	Video error analysis, minimum case	59
Figure 22	Typical 3-point data spread	61
Figure 23	Typical 5-point data spread	63
Figure 24	Typical 7-point data spread	65

LIST OF SYMBOLS

g	Peak Deceleration (G's)
p.s.i	Pounds per Square Inch static loading of cushion
v	Impact Velocity of test platen
G	Acceleration due to gravity (386.4 in/sec^2)
h	Equivalent Drop Height
Pixel	The size of 1 display dot on the CRT screen
Y	Cushion Displacement at time n
s	Sampling Time Seperation (3 msec in this study
P	Conversion of Inches/Pixel
T	Cushion Thickness
s-L	Static Loading of cushion
t	Time

CHAPTER 1

INTRODUCTION

Cushioning is often the only way to protect a product many situations. If a product is not sturdy enough to withstand the rigors of the distribution environment by itself. some form of protection, hereafter refered package cushioning, is generally required. to However, since package cushioning can be expensive and depends on product fragility, it is important to use only enough cushioning to adequately protect the product. For a given packaging material and product fragility it can be shown that a trade off generally exists between the cost of excessive packaging and the cost of excessive damage. This is shown in figure 1. Ideally, the amount of protection built into a package should just make up for the difference between the hazards of the environment and the ability of the product to withstand these hazards. This is graphically illustrated in Figure 2. If the product can withstand rigors of the distribution environment, no the cushioning is needed. The product's fragility may be procedure outlined in ASTM determined using the procedure D-3332 [1]. The hazards of the distribution environment may be determined using measurement techniques on actual test shipments of the product

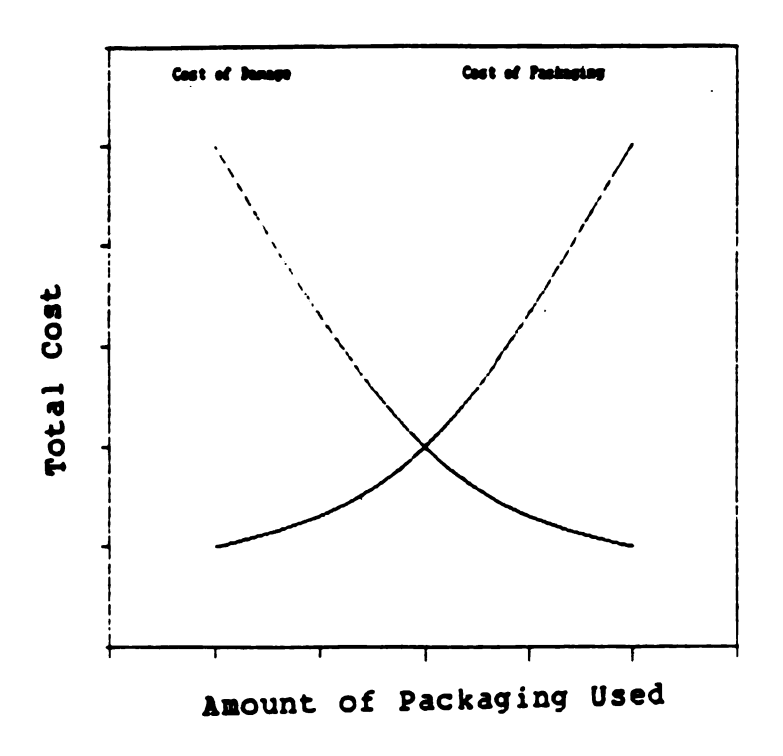


Figure 1. Trade-off between package costs and damage costs.

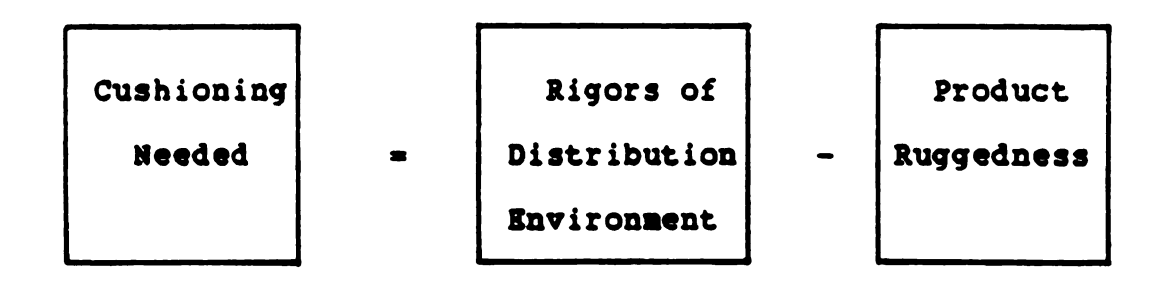


Figure 2. Methodology for determining cushioning needed

[2,3,4]. This allows for the amount of package protection required to then be determined.

The function of a cushion is to protect a fragile product by dissipating the free fall energy accumulated in a drop more slowly than would be dissipated in an unprotected drop. This energy is dissipated by a number of mechanisms such as heat transfer from the air in the cushion to the surrounding cell structure (5), damping (6), and plastic deformation of the cushioning material (7). The peak deceleration in the impact is commonly used as a measure of cushion effectiveness. A larger peak deceleration indicates that the free fall energy is dissipated too rapidly and therefore, less protection is offered.

The standard method of portraying the protection potential of a cushion in an impact is the "cushion curve" as shown in figure 3. A cushion curve relates cushion thickness, load bearing area, and product weight to the peak deceleration (g's) that can be expected in a free-fall drop from a certain height. The method for generating cushion curves can be found in ASTM procedure D-1596 [8]. As the material properties of a cushion often change somewhat with repeated drops,

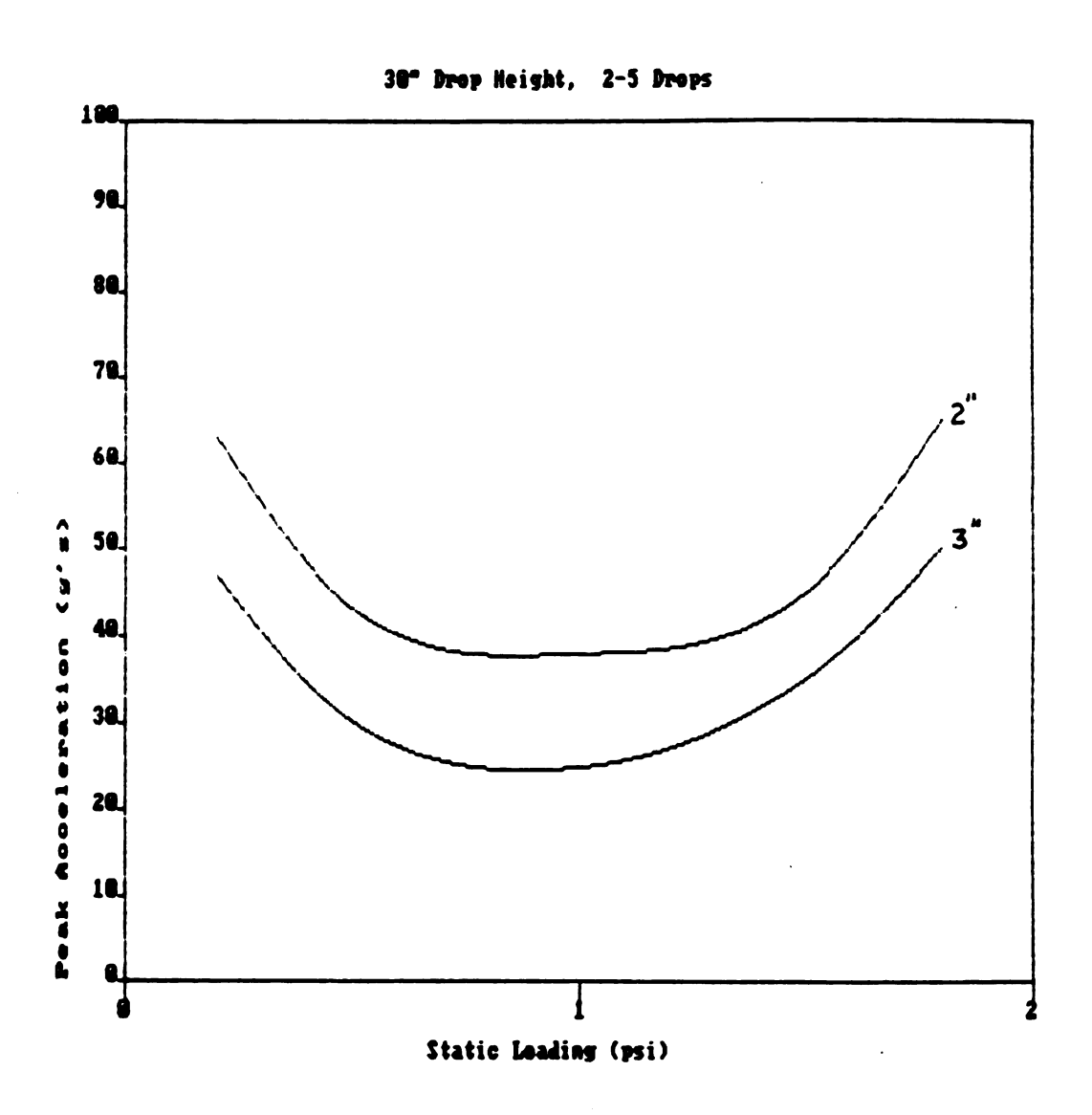


Figure 3. Typical Cushion Curve

the cushion curve will depend on the number of drops. The curves most often used in actual package design are the '2 - 5 drop' curves which represent the average deceleration experienced for the 2nd, 3rd, 4th, and 5th impacts under the same conditions. For this reason, the results of this study will be presented in the standard format of cushion curves, with static loading (P.S.I.) on the X-axis, and shock (g's) on the Y-axis. The curves generated from the video results will then be compared to published cushion curves for '2 - 5 drops' at the indicated drop height. The results should not be interpreted as new cushion curve data to be used for design purposes. This format is used merely for comparison purposes.

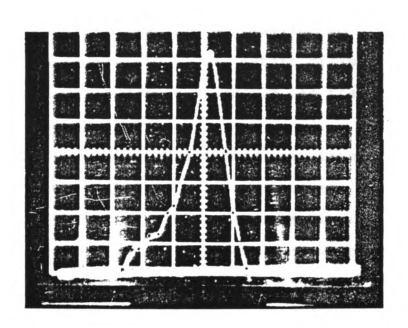
The standard method for developing a cushion curve requires some technique for measuring the peak deceleration during the cushioned impact. There are many used to measure this. Mechanical shock measuring devices include spongy balls, cantilevered beams, and in general any spring-mass system whose response to shock can be measured and translated into peak deceleration. The problem with all mechanical devices is that their response is slow and is determined to a great extent by the duration of the shock [9]. The

response time of a spring-mass type of mechanical accelerometer is governed by its natural frequency. If the response time is comparable to the shock duration, then the mechanical accelerometer will provide useless results. Only mechanical accelerometers with natural frequencies that are high enough to avoid this problem will produce accurate results. The piezo-electric accelerometer is such a device which relies on the deformation-dependent electrical properties of a crystal to measure deceleration. In spite of the widespread use of these types of accelerometers, they are still plaqued with problems, some of which are outlined below:

that produce minute voltages in proportion to the forces they are subjected to. Since force is proportional to acceleration through Newton's Law, the voltage produced becomes a measure of the deceleration experienced. While relatively reliable, they nevertheless require calibration to determine the ratio of voltage output to the deceleration experienced. The accuracy of the results will depend on the technique used and the

skill of the operator, which makes exact calibration difficult.

- 2. CONNECTION IMPEDANCE: If an accelerometer is not properly connected to the test item, inaccurate measurements will result. The high strains generated when the impact occurs may alter the electrical resistance of the connection. This may alter the output voltage and introduce an error in the measured deceleration.
- 3. COUPLER ERRORS: A piezo-electric accelerometer requires a capacitance coupler in order for an oscilloscope to measure the output. This coupler has an associated error. Also, as in #2 above, the connections to and from the coupler may induce an error. The power source for the coupler may magnify this error.
- 4. OSCILLOSCOPE ERRORS: Since the trace width of the accelerometer signal displayed on an oscilloscope is typically on the order of 1 mm at the very least, the peak height of the trace will be in error by this amount. See Figure 4. In addition,



The divisions in the photo are each l cm x l cm. The width of the shock pulse trace is appx. l mm (determined visually).

The settings for the oscilloscope in this photograph were 5 ms/division horizontally, 20 mw/division vertically. The drop height was 42", the static loading 1.0 p.s.i., and the cushion sample tested was 3" thick Bthafoam 220. The sensitivity of the accelerometer used was 2.0 mw/g (see Appendix D).

Figure 4. Typical shock pulse recorded by an accelerometer

the oscilloscope itself has inherent errors such as drift (the gradual shifting of the ocsilliscope's beam over time), connection errors, and calibration errors. The user may also induce an additional error by failing to differentiate between the base line (start of impact) and the peak (maximum deceleration) on the trace.

- 5. AMBIENT ERRORS: Electromagnetic interference from overhead lights. power sources. and nearby can induce a current in the cable equipment through induction, the result of which is to alter the signal from the accelerometer. This may be minimized but completely eliminated by not shielding the cables or reducing nearby electrical activity in the environment. An improper ground loop between equipment may also result in Temperature variations may cause errors in virtually all of the equipment involved due to temperature dependent electrical properties of the of electrical components found in the types equipment.
- 6. TRIBO-ELECTRIC NOISE: Since the signal cable cannot be entirely immobilized throughout the

impact, cable flexing will alter the signal. This error can be reduced by using a signal cable with no more slack than necessary for the operation of the test equipment.

- 7. TRANSVERSE ACCELERATION ERRORS: Accelerations not confined to the axis of the accelerometer will cause an output error. These can be reduced by maintaining alignment of the accelerometer in the vertical direction during impact and by using well-braced mounting and proper test equipment.
- 8. OFFSET DUE TO DAMAGE: When overloaded with accelerations beyond their measurement capabilities, accelerometers may be permanently affected in the form of an offset from the calibration value. While this error can prevented through careful handling of accelerometers, it is often impossible to know the complete handling history of an accelerometer beforehand.
- 9. RINGING OF THE TEST FIXTURE: During impact, the test fixture and associated support equipment will

ring, or vibrate at their natural frequencies. This causes transverse vibrations which affect the signal from the accelerometer and lessen the impact by dissipating some of the impact energy which the cushion would otherwise have to absorb. This effect may be reduced by eliminating free play within the equipment as much as possible. If this is not possible, the output of the coupler may be electronically filtered to take out the undesirable frequency components in the high signal associated with externally induced noise, transverse accelerations, and fixture ringing. The positioning of the accelerometer can also effect the transmitted shock pulse.

Taking into account all of the above possible sources of error, the accelerometers used to generate deceleration data are likely to give results which are accurate to ± 14 %. This figure was calculated as outlined in Appendix B.

As mentioned earlier, some of the sources of error may be removed electronically through filtering. The remaining sources of error still exist however. For this reason, a new method for determining the peak deceleration in cushioned drops is desired.

The purpose of this study is to compare the peak deceleration obtained in an impact in a cushioned free-fall drop using a piezo-electric type accelerometer to the peak deceleration obtained using the high-speed video method outlined in Chapter 2. Although certain test conditions were used, it is not the intent of this study to generate any conclusions about the cushioning materials based on the results obtained under these conditions. Rather, the intent is to compare the two methods under the same set of arbitrary test conditions.

CHAPTER 2

A NEW METHOD

This chapter evaluates a new and simpler visual method for determining the deceleration in a cushioned impact. The technique uses a real time plot of product displacement versus time obtained from a high-speed video camera. The camera used in this research was a Kodak Ectapro 1000 which is capable of capturing images seperated by 1 millisecond intervals (Fig. 5). When a suitable mathematical function is fitted to this discrete displacement vs. time data, the deceleration function may be obtained as the second derivitive of the displacement function. This method offers several key advantages over the conventional accelerometer method, such as:

- NO CONNECTION ERRORS: The very nature of the video recording system eliminates connection errors by eliminating the connections themselves.
- 2. NO COUPLER ERRORS: There is no coupler.
- 3. NO TRIBO-ELECTRIC NOISE: Again, there is no physical connection to the test sample. This of

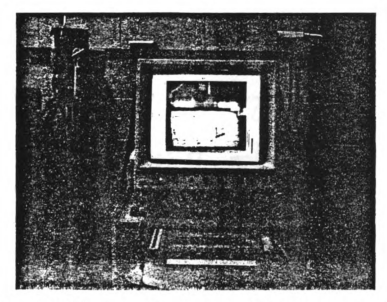


Figure 5a. Cushion as it appears before compression.

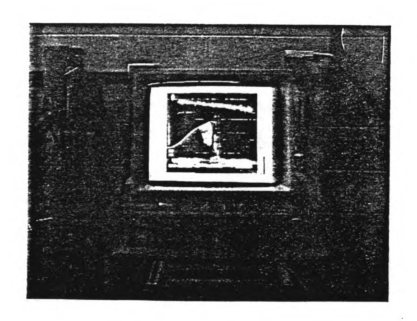


Figure 5b. Cushion as it appears during compression.

Figure 5. View screen of Kodak's Ectapro 1000 system.

course assumes that the cable between the camera and recorder does not move appreciably during the shock.

- 4. FEWER AMBIENT ERRORS: Ambient conditions can only effect the high-speed video recording system and this possibility has been reduced by the manufacturer by enclosing the electronics of the recording system in a metal enclosure (a Faraday Cage) which essentially eliminates electromagnetic interference.
- 5. NO TRANSVERSE VIBRATION ERRORS: The high speed video system may be used to analyze motion in one direction only by orienting the camera so that the on-screen grid system coincides with this direction.
- 6. NO RINGING ERRORS: Unless the amplitude of vibration of the test fixture is greater than the resolution of the camera (approximately .03"), which is rarely the case, the displacement measured by the camera will be essentially that of the product on the cushion.

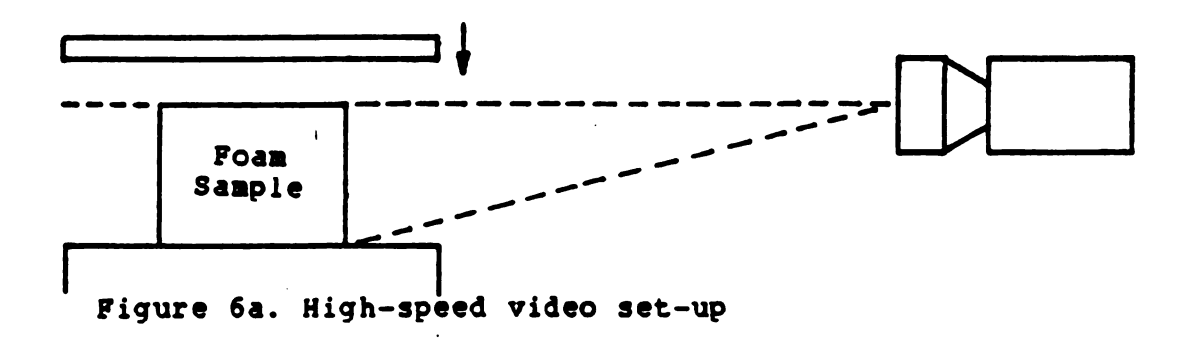
7. NO ADDED MASS: Even though present day accelerometers relatively light-weight. are certain applications are precluded because of their weight. An example would be measuring the dynamic characteristics of thin films. The highspeed video method is ideal for such applications.

In spite of the obvious advantages, there are disadvantages, few of which however affect the accuracy of the technique. These include:

- 1. HIGH COST: The current price of the necessary test equipment is around \$80,000, far greater than the cost required for all of the equipment used in the accelerometer method. This limitation can be expected to decrease as high-speed camera technology and use improves.
- 2. LIMITED USAGE: Because of the strict set-up requirements of the high-speed video system, this technique is limited to laboratory use only except in special cases.

- 3. FREQUENCY CUT-OFF: Since the video system has a maximum "capture speed", displacement resolution decreases with increasing speed of the event to be captured. This limiting capture speed effectively acts as a low-pass filter which eliminates high-frequency motion superimposed on the dominant compression/expansion motion during the impact. This limitation may actually be regarded as an advantage since it automatically eliminates ringing problems with the test fixture.
- RESOLUTION: The amount of detail. 4. CAMERA displacement resolution, of the camera will limit its accuracy. Movements less than the resolution of approximately .03" for the camera used here cannot be accurately displayed as this is the approximate size of a "pixel" on the video screen. This becomes critical around the displacement, when the change in displacement is less than the camera resolution. This most likely accounts for the greatest source of error in the method. A possible solution would be to focus in on the lower 1/3 of the cushion in order to record the critical moments during peak only displacement.

- 5. SCREEN ERRORS: Both image blurring and reading errors also limit the accuracy. Blurring may be minimized by proper lighting and adequate camera speed. In the tests performed here, the speed of the Kodak video system was adequate but less than optimal. This resulted in occasional blurring at critical moments during measurement. It may be assumed that some degree of reading error was also present.
- 6. ANGULAR OFFSET: Since the camera must capture continuous motion through a range of elevations, must film at an angle most of the time. The actual displacement will therefore be distorted by the changing camera angle. Angular offset tends to make the perceived compression about 2% greater than the actual compression. This is illustrated Figure 6. This may be minimized during the critical moment of peak displacement by adjusting the height of the camera lens to that of the bottom of the test cushion. In any event, if necessary this error can be removed by using trigonometric principles. See Figure 6. This error will not be present at all if the dimension of the cushion sample being tested is the same



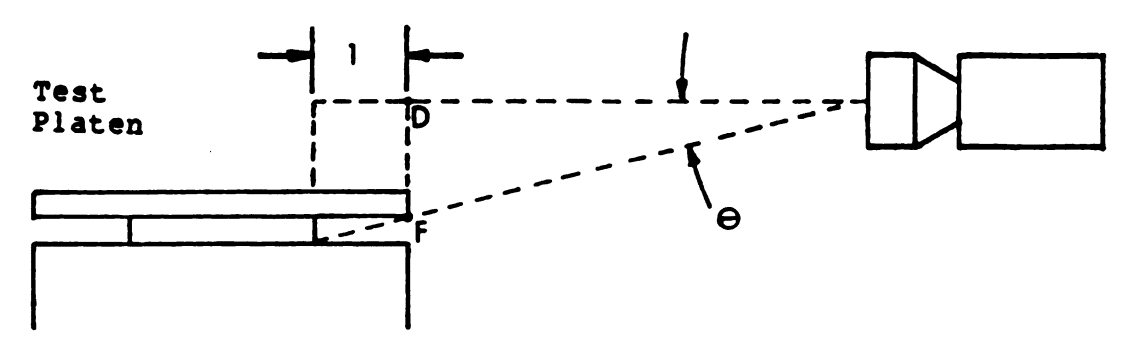
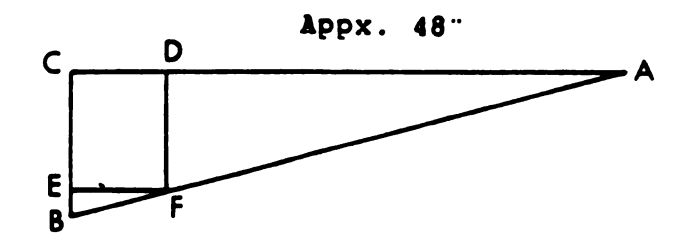


Figure 6b. Test platen interference



Line DA = Distance of camera to sample = 48"

Line EF = CD = Distance from platen edge to sample = 1"

Line DF = Perceived compression

Line BC = Actual compression

Therefore, Actual Compression = 1.02 x Perceived Comp.

Figure 6c. Trigonometric error analysis

Figure 6. Illustration of angular offset error

from front-to-back as the test platen.

7. GROUND-BORN VIBRATIONS: Vibrations of sufficient magnitude transmitted through the ground to the camera by the force of the impact can cause the camera's aperature to move. This could result in a displacement error which can be minimized through the use of a proper seismic mass to anchor the test equipment and by isolating the camera from the ground.

To utilize the high-speed video method in determining the peak deceleration experienced during a cushioned drop, the following equipment and materials are needed;

TEST MATERIALS

Although the test samples may be any material of a resilient nature, as described in ASTM D-1596 [8], the material used in these tests was Ethafoam 220, a product of Dow Chemical Company. Test samples are usually 8" x 8" x Thickness, but for these tests, it was necessary to reduce the surface area to 6" x 6" to reach the upper static loadings used.

TEST APPARATUS

The test apparatus used was a model 23 free-fall drop tester manufactured by Lansmont. A piezoelectric accelerometer mounted to the platen was used in conjunction with a digital storage oscilliscope to record the shock pulse. This set-up is illustrated in Figure 7. A Kodak Ectapro 1000 high-speed video recording system was used to gather the displacement versus time data. The camera was set up so that the entire compression range of the cushion from first contact to maximum deformation was within view of the camera lens. This is shown in Figure 8.

TEST PROCEDURES

The procedure to record a single drop using the highspeed video method is as follows;

1. RESET VELOCITY DETECTOR ON DROP TESTER: This is standard on most drop testers in order to ensure that the proper impact velocity is reached for the desired free fall drop height.

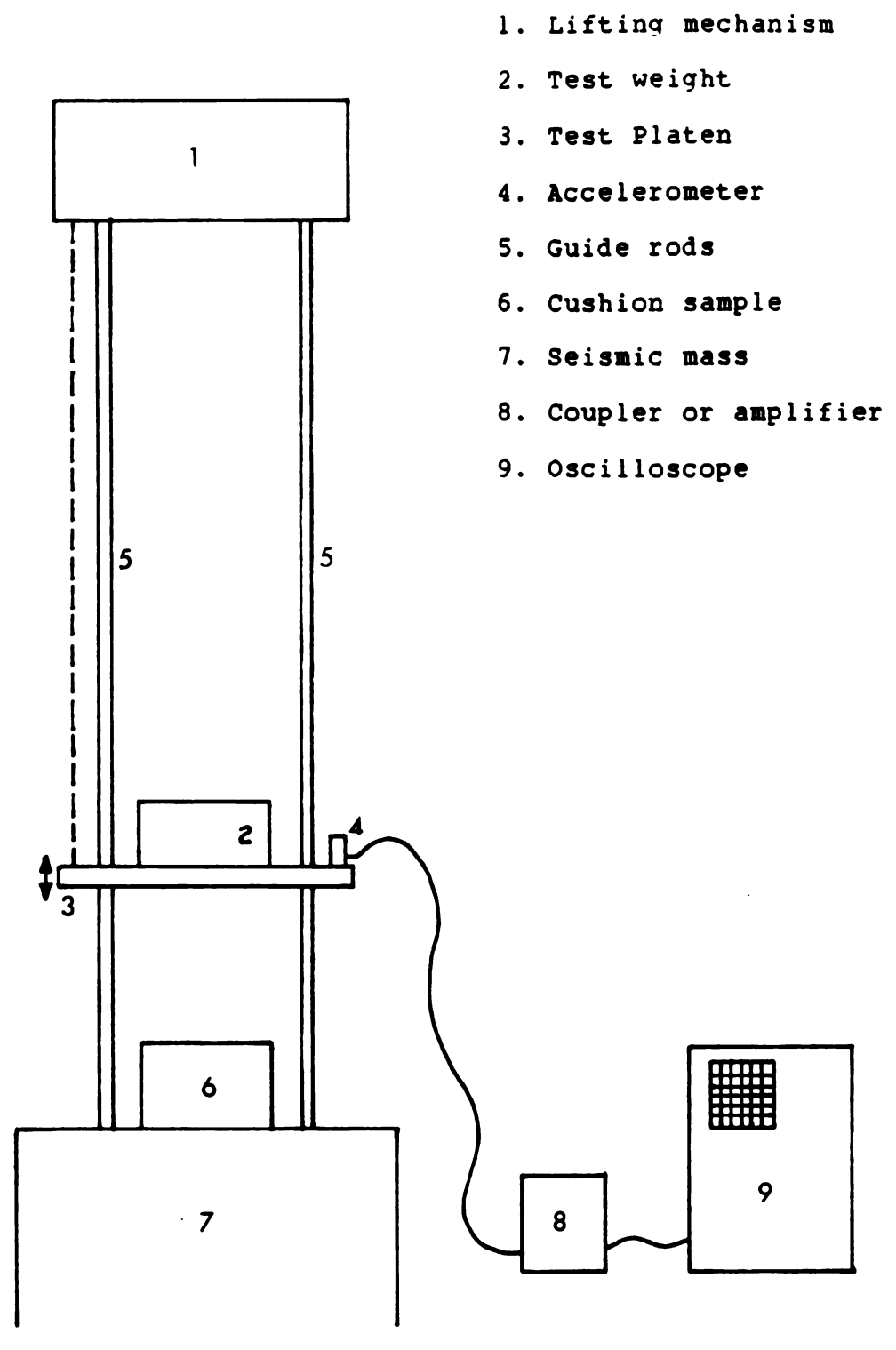


Figure 7. Test set-up for the accelerometer method.

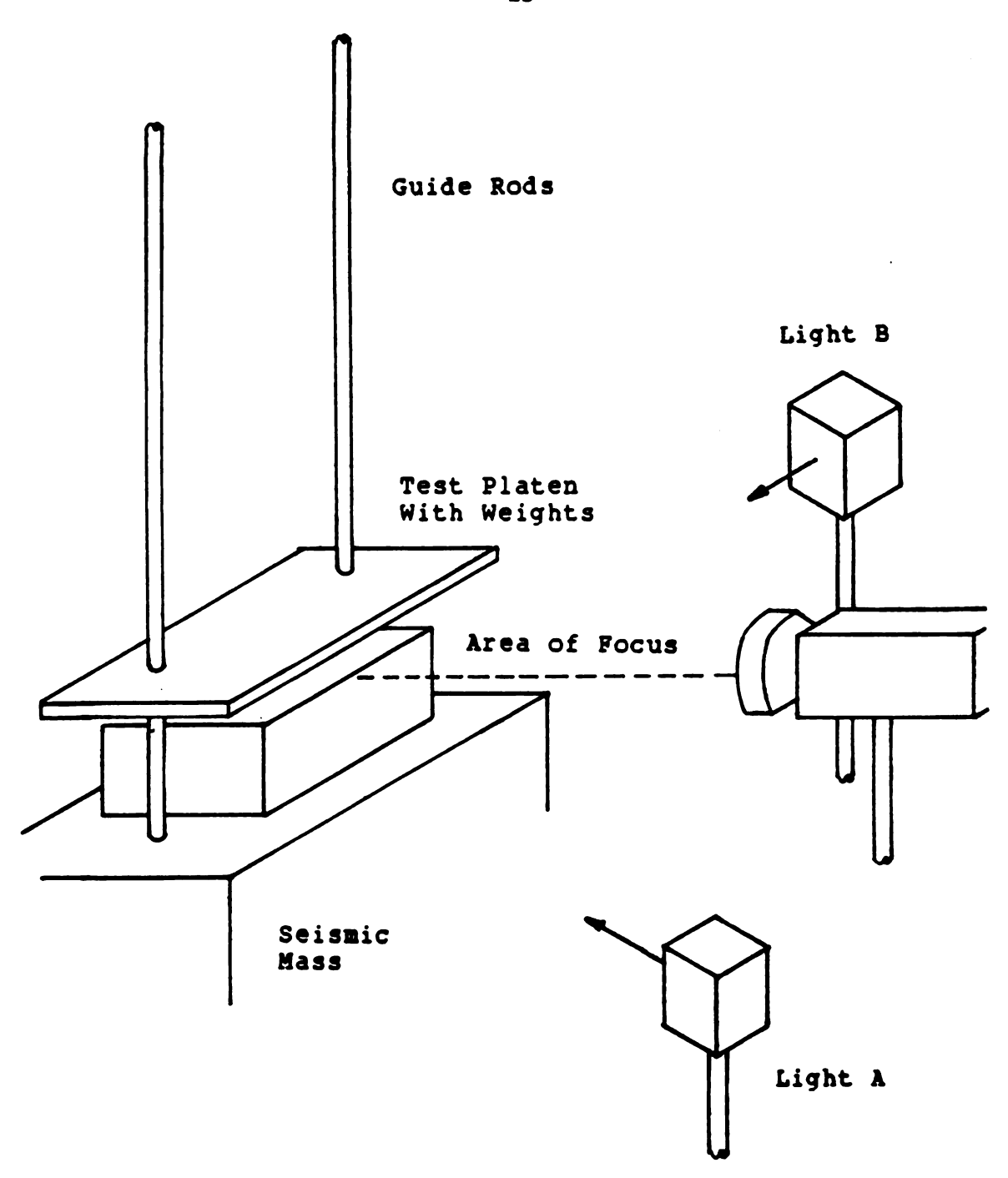


Figure 8. Test set-up for the high-speed video method

- 2. RESET STORAGE OSCILLISCOPE: (optional) The use of a storage oscilliscope is required only if it is desired to compare the result with that obtained from an accelerometer.
- 3. TURN ON CAMERA LIGHTS: The high-speed camera requires very bright lighting for proper filming.
 As such lights are very hot, it is desirable to leave them on only when required for filming.
- 4. ADJUST CAMERA POSITION: In the "live" or camera-on mode, the view can be lined up precisely. This should be checked before each drop to avoid possible loss of data due to an accidental bump to the camera. At this time the optimum focus can also be obtained.
- 5. START HIGH-SPEED CAMERA RECORDING: The high-speed camera uses up video tape very quickly. When running at the speed used in these experiments (23 ft/sec), a single tape can hold approximately 30 seconds of real-time data. For this reason it is desirable to film as little as possible for each drop.

- 6. INITIATE DROP TEST: Self explanatory.
- 7. TURN OFF HIGH-SPEED CAMERA: See #5 above.
- 8. TURN OFF CAMERA LIGHTS: See #3 above.
- 9. READ VELOCITY DETECTOR: This is done to verify that the impact velocity was correct for the desired free fall drop height, where;

$$V_i = \sqrt{2Gh}.$$
 (Eq.1)

- 10. READ OSCILLISCOPE: Optional, see #2 above.
- 11. TRANSCRIBE CUSHION DISPLACEMENT DATA: The highspeed video system used was equipped with a cursor
 location readout system which allows for
 measurements of events to within l pixel (.03"
 for these tests). By selecting a reference point,
 such as the test platen edge, the displacement of
 this point can then be measured to within .03" at
 l millisecond intervals. Continue measurements
 throughout the displacement cycle, noting where
 the peak displacement occurs. Since the read-out
 system measures displacement in pixels, these

values can be converted to inches only after the entire sequence is viewed.

12. PICKING DATA POINTS: The mathematical analysis used here requires that displacement data be sampled at regular time intervals. There should be the same number of points on either side of the peak displacement, determined upon viewing the recording. In these tests, the sampling time interval used was 3 milliseconds. A typical transcription of the data appears in Figure 9. This method requires a conversion from pixels to inches. To determine this, one must measure the thickness of the sample cushions before testing. After the video record has been made, the reticle location system can be used to determine the locations for the top and bottom of the cushion on screen. The value for inches per pixel can then be determined as shown in Figure 10 and determined as follows:

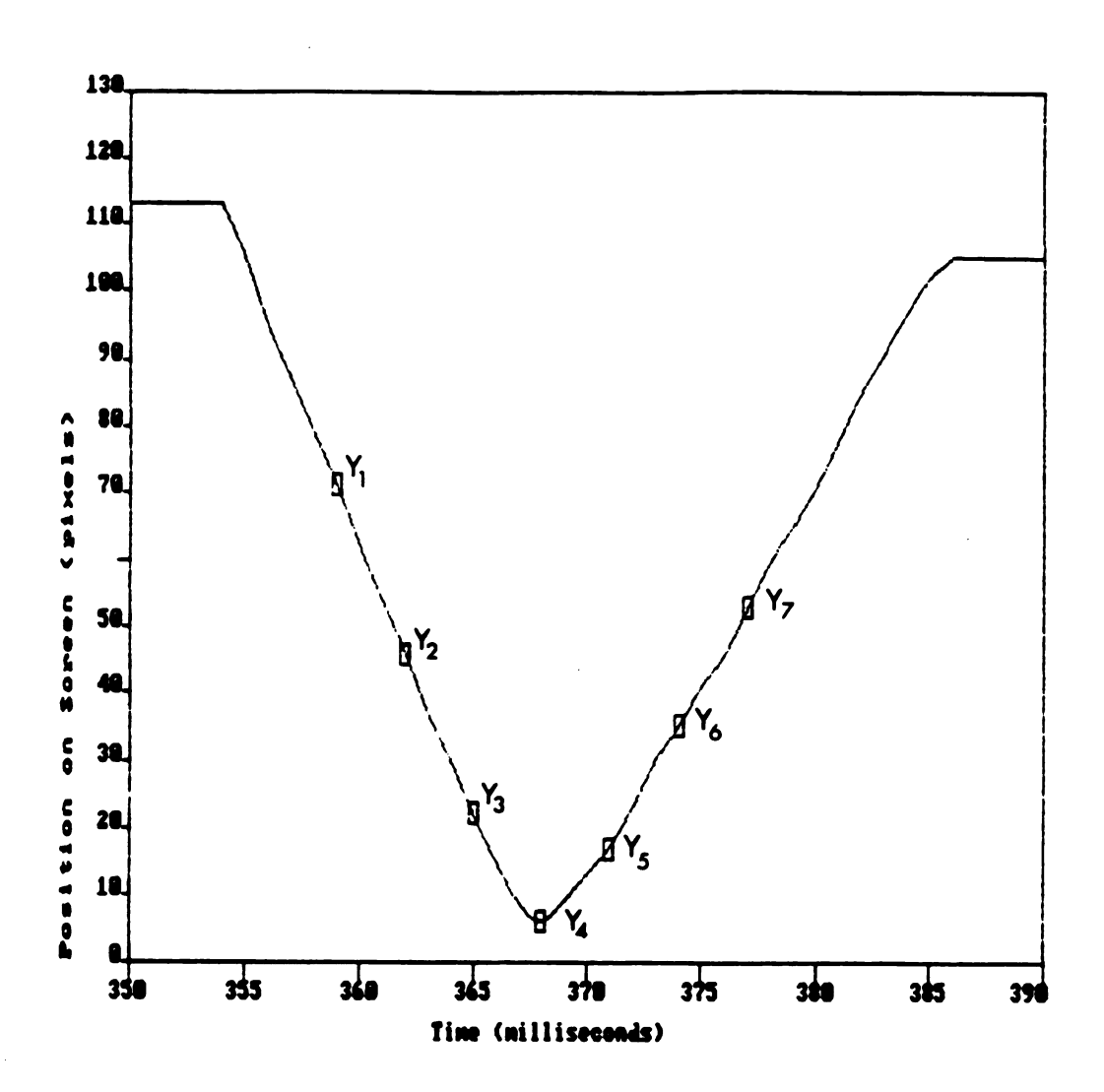


Figure 9. Typical displacement plot of cushion compression

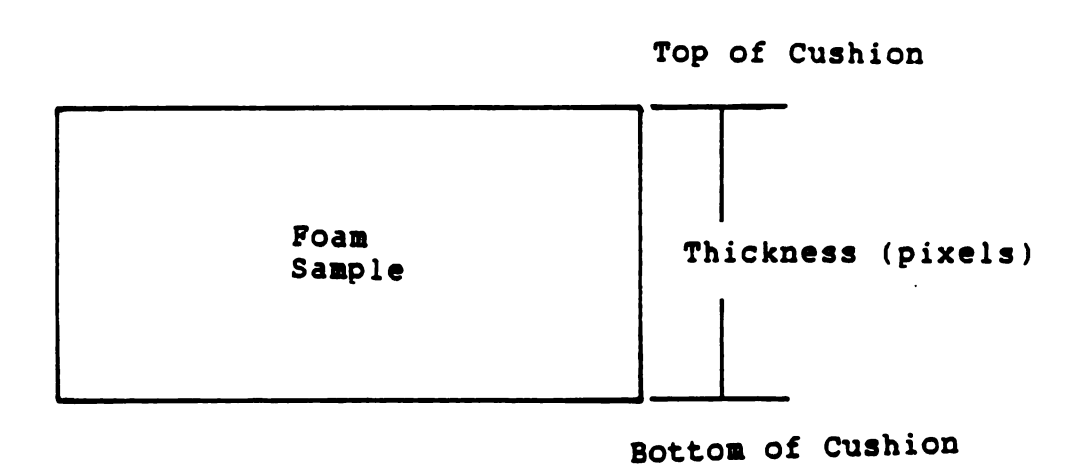


Figure 10. Determination of P (inches/pixel) from sample

Table 1. Values of inches/pixel calculated in study

30" drop height, 2" cushion	.024 in/pixel
36" drop height, 2" cushion	.024 in/pixel
42" drop height, 2" cushion	.026 in/pixel
30" drop height, 3" cushion	.032 in/pixel
36" drop height, 3' cushion	.031 in/pixel
42" drop height, 3" cushion	.030 in/pixel

involves fitting a polynomial function to any number of displacement versus time data points. For greater accuracy, such a spline was fitted to the 7 equally spaced data points obtained in \$12 and shown in Figure 9. Such a function represents the displacement of the cushion over time during the impact, and its second derivative is the instantaneous acceleration. The details of the derivation are carried out in Appendix C and the result is that the peak deceleration experienced during the impact in terms of the displacement values Y1, Y2, ...etc in pixels taken at evenly spaced intervals t seconds apart is;

(Eq.15)

$$g = \frac{2(y_1)-27(y_2)+270(y_3)-490(y_4)+270(y_5)-27(y_6)+2(y_7)}{180(s^2)(386.4 \text{ in/sec}^2)(P)}$$

See Appendix C for the derivation of this equation.

for this study, s was .003 seconds. The values for inches/pixel are shown in table 1. This value is also the effective resolution of the system, as discussed earlier in disadvantage #4. The value for inches/pixel changed from test-to-test due to camera relocation between most tests. Therefore, it was calculated for every drop test recorded. This procedure is illustrated in Figure 10.

The procedure for recording a single drop using the accelerometer method is detailed in ASTM D-1596 [8].

Tests were conducted using the above procedures to determine how closely the results of the high-speed video method compared to the results obtained from the accelerometer method. The following test conditions were used.

P.S.I. were used. This represents the upper range of static loadings that are normally used in cushion design and was singled out for testing not only for this reason but also since accelerometers are likely to have the greatest difficulty in gathering data under these high G conditions. Since the static loadings were

chosen to be in this upper range, a smaller than normal cushion sample size was required due to the weight limitations of the test equipment used. The cushion size used was 6"x6" and the weights and static loadings produced are shown in Figure 11.

DROP HEIGHTS: Actual drop heights of 30",36", and 42" were chosen since they are typical of industry cushion curves. The distance the test platen actually falls during the tests must be made somewhat higher than these values since friction between the guide rods of the drop tester and the test platen slow the test platen down as it falls. For this reason, an impact velocity gate was utilized to set the platen drop heights so that the desired free fall drop heights listed above were achieved. The platen drop height is adjusted until the target impact velocity for each of the drop heights is achieved

Impact Velocity $(V_i) = \sqrt{2Gh}$ eq.(1)

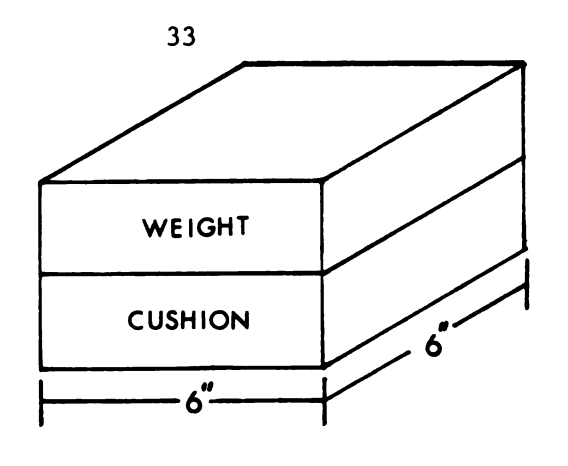


Figure 11. Weights and static loadings used in tests

For the desired test drop heights of 30", 36", and 42" the required impact velocities are 152 inches per second, 168 inches per second, and 180 inches per second respectively.

SAMPLE CHARACTERISTICS: The samples used were 6 x 6 blocks of Ethafoam 220, a low density expanded polyethylene foam weighing 2.2 pounds per cubic foot made by Dow Chemical. Two and three inch thick cushions were chosen as typical thicknesses that would be used in industrial applications. Twice as many samples were constructed as needed for the testing and checked for accurate measurements. Any samples that failed to meet specifications were discarded. From the remaining samples, the actual test samples were chosen at random for each drop.

TEST REPETITIONS: In order to maintain a minimum degree of statistical significance, two repetitions of each test condition were performed. While this is perhaps insufficient to gather statistically valid data for plotting cushion curves, it was judged to be adequate for the comparison between the accelerometer and the video methods since both acceleration measurements were taken simultaneously during the same

drop. This allowed for a direct comparison of the results as conditions were identical for each method.

These test conditions are summarized in Figure 12.

Test Drop Heights	3	30", 36", 42"
Test Static Loadings	4	1.0, 1.5, 2.0, 2.5 p.s.i
Test Sample Dimensions	2	2" x 6" x 6"
		3" x 6" x 6"
Test Samples	1	Ethafoam 220
Test Repetitions	2	

Total Drop Tests 48

Figure 12. Summary of test conditions

CHAPTER 3

DATA & RESULTS

The data for the displacement versus time observations obtained as described in step #12 of the high-speed video method can be found in Tables 5 and 6. This data can be used in Equation 15 to calculate the instantaneous acceleration values. The data obtained by using an accelerometer to measure the peak deceleration can be found in Tables 7 and 8.

The results of both methods are compared directly in Tables 2 and 3, and the data is displayed again in the format of cushion curves in Figures 13 through 15. Cushion curves generated from the data provided by the Dow Chemical Corporation are shown in Figures 16 through 18.

Table 2. Results of both methods using 2" cushions.

h	/	T	/	S-L	Video Method	Accelerometer Method
30"	/	2	/	1.0 psi	98 g's 89 g's	95 g's 76 g's
30	/	2	/	1.5 psi	140 g's 139 g's	143 g's 140 g's
30"	/	2	/	2.0 psi	185 g's 185 g's	175 g's 178 g's
30	/	2	/	2.5 psi	203 g's 203 g's	255 g's 260 g's
6"	/ 2	2 ··· .	/ 1	l.0 psi	129 g's 146 g's	105 g's 113 g's
6° .	/ 2	2 ·· .	/]	l.5 psi	226 g's 201 g's	280 g's 275 g's
36"	/	2	/	2.0 psi	236 g's 246 g's	310 g's 325 g's
36"	/	2	/	2.5 psi	302 g's 255 g's	460 g's 460 g's
42"	/	2	/	1.0 psi	159 g's 166 g's	140 g's 158 g's
42"	/	2	/	1.5 psi	286 g's 226 g's	350 g's 345 g's
42"	/	2	/	2.0 psi	256 g's 235 g's	430 g's 430 g's
42"	/	2 ··	/	2.5 psi	304 g's 284 g's	590 g's 570 g's

h = equivalent drop height in inches
T = cushion thickness in inches

S-L = cushion static loading in p.s.i.

Table 3. Results of both methods using 3" cushions.

h	/	T	/	S-L	Video Method	Accelerometer Method
30"	/	3	/	1.0 psi	48 g's 46 g's	36 g's 35 g's
30	/	3	/	1.5 psi	43 g's 16 g's	47 g's 44 g's
30 "	/	3	/	2.0 psi	65 g's 52 g's	63 g's 65 g's
30"	/	3	/	2.5 psi	85 g's 75 g's	103 g's 93 g's
36"	/	3	/	1.0 psi	82 g's 106 g's	50 g's 54 g's
36"	/	3	/	1.5 psi	146 g's 147 g's	93 g 's 90 g 's
36"	/	3	/	2.0 psi	169 g's 133 g's	118 g's 110 g's
36	/	3	/	2.5 psi	190 g's 189 g's	158 g's 163 g's
42"	/	3	/	1.0 psi	101 g's 99 g's	57 g's 63 g's
42"	/	3 ·	/	1.5 psi	171 g's 183 g's	125 g's 135 g's
42"	/	3	/	2.0 psi	179 g's 202 g's	160 g's 168 g's
42"	/	3	/	2.5 psi	236 g's 200 g's	245 g's 235 g's

h = equivalent drop height in inches
T = cushion thickness in inches

S-L = cushion static loading in p.s.i.

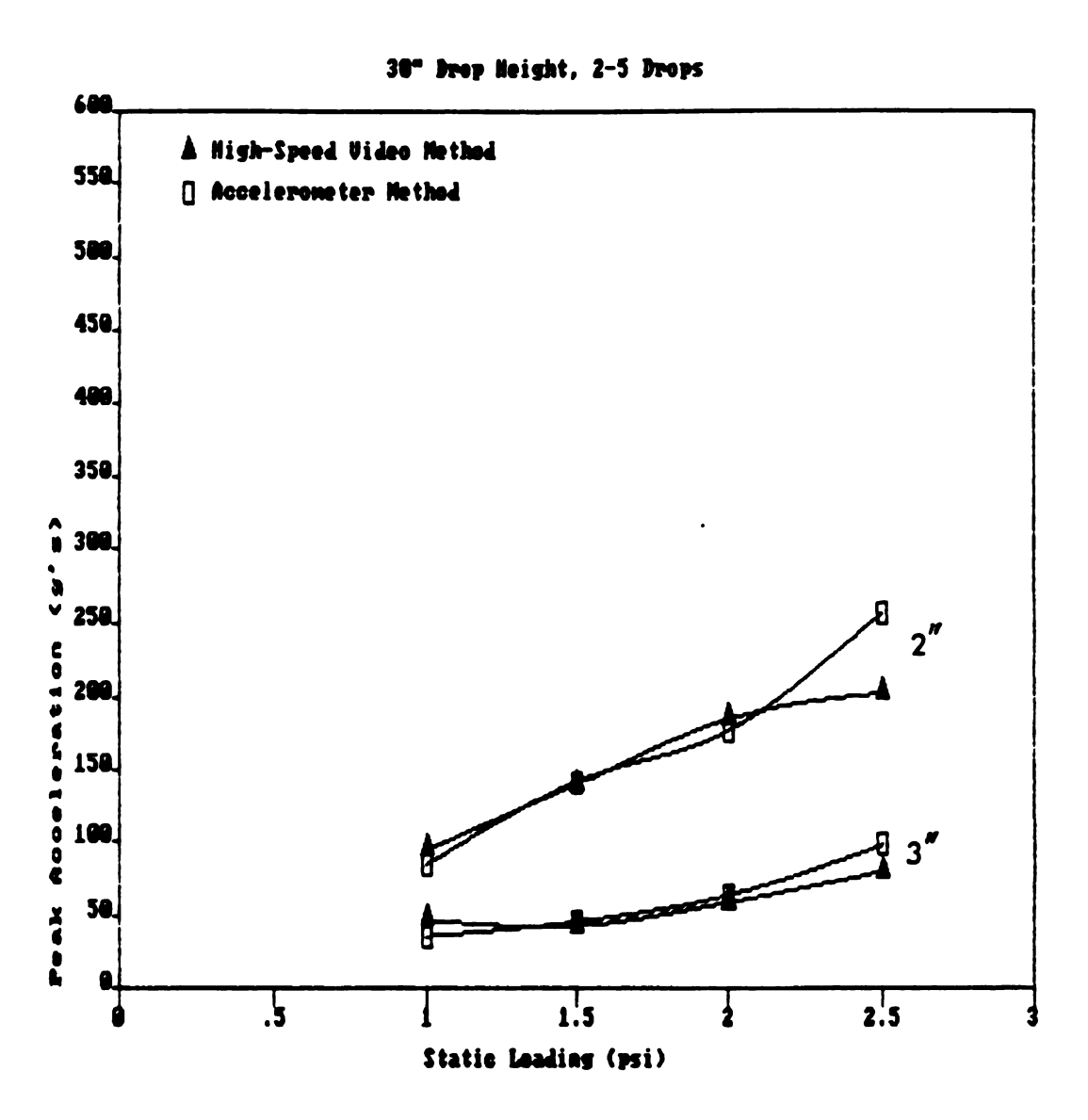


Figure 13. Results of both methods at a 30" drop height

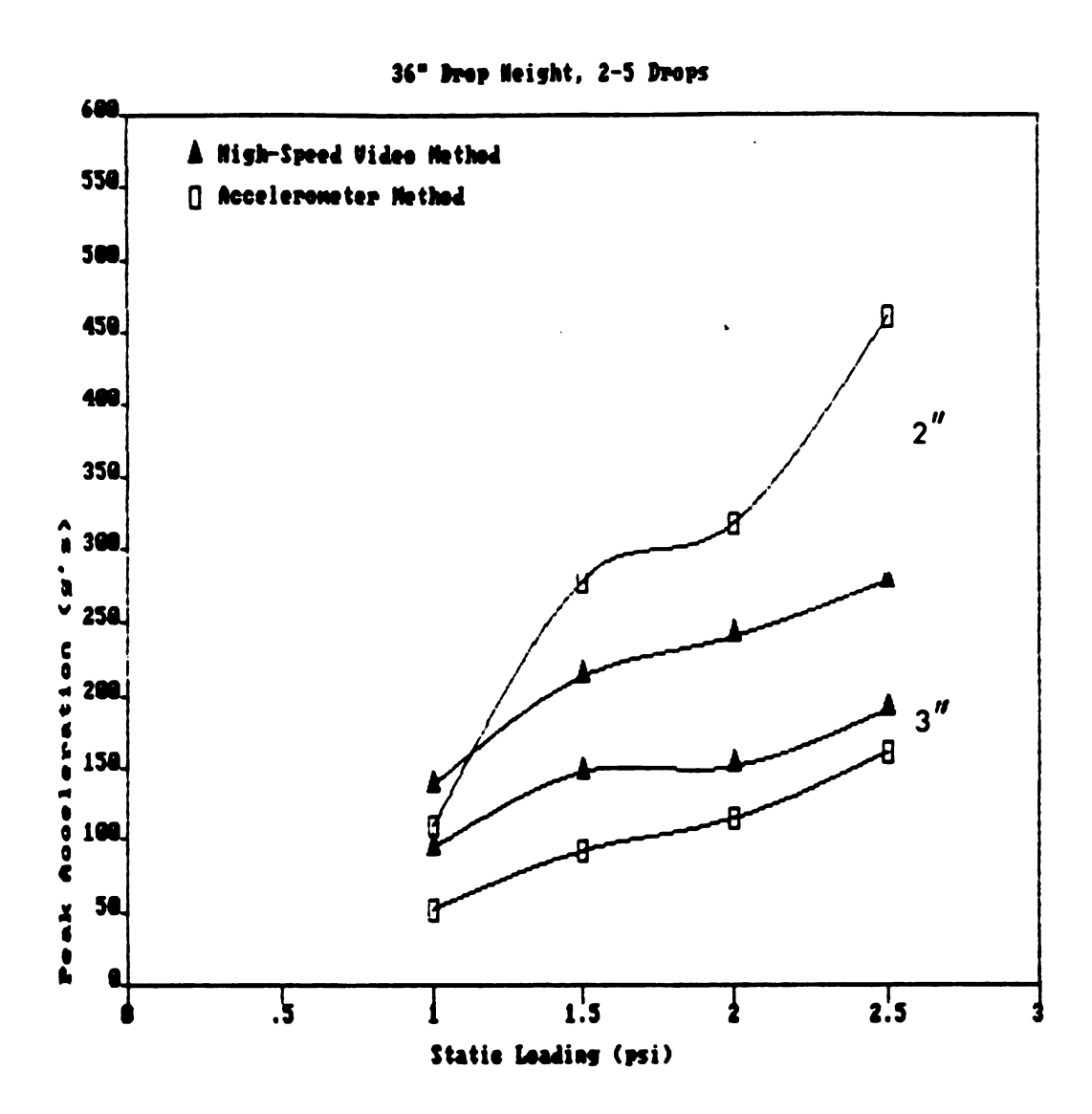


Figure 14. Results of both methods at a 36" drop height

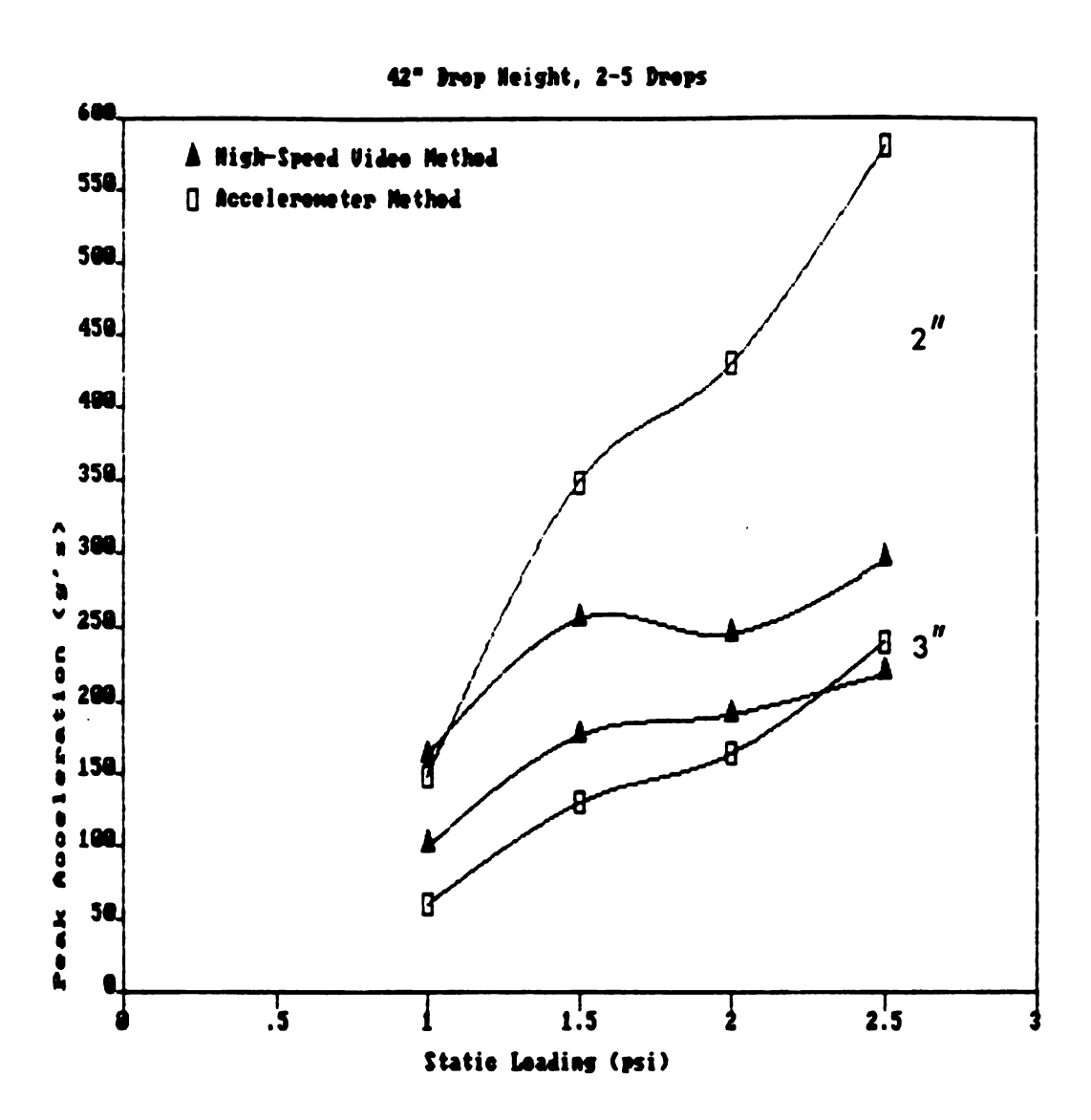


Figure 15. Results of both methods at a 42" drop height

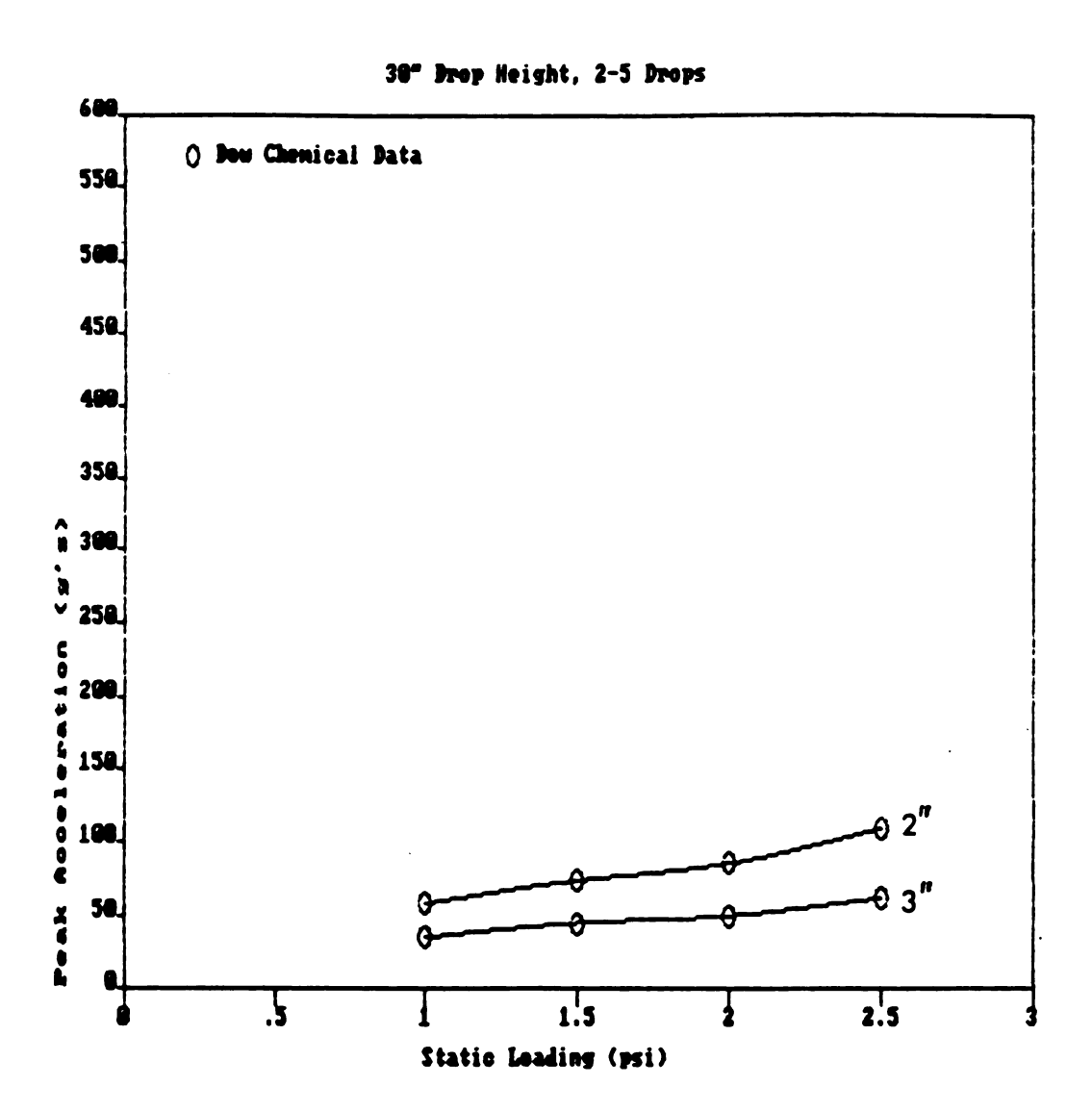


Figure 16. Dow Chemical Co. data for a 30" drop height

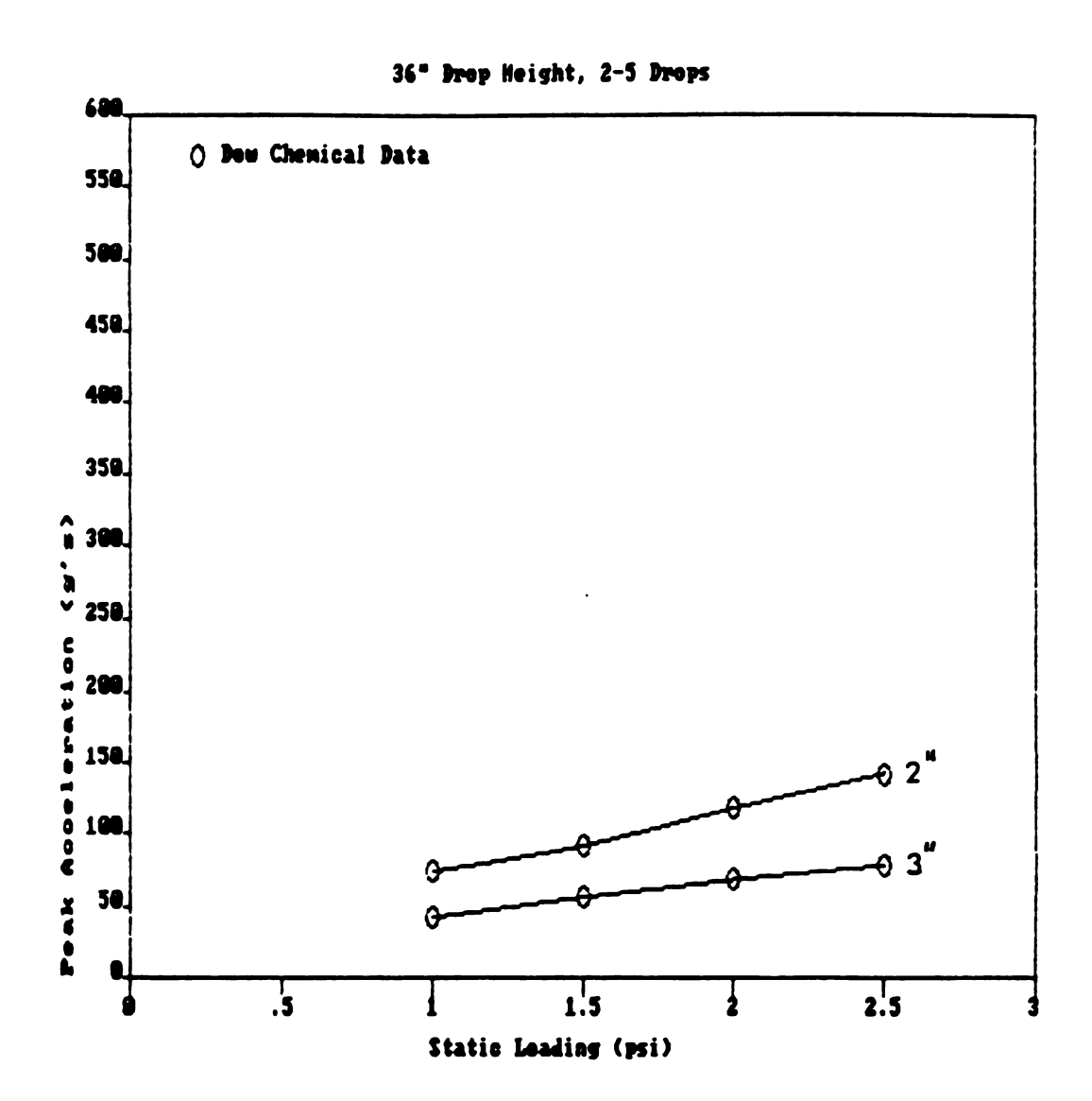


Figure 17. Dow Chemical Co. data for a 36" drop height

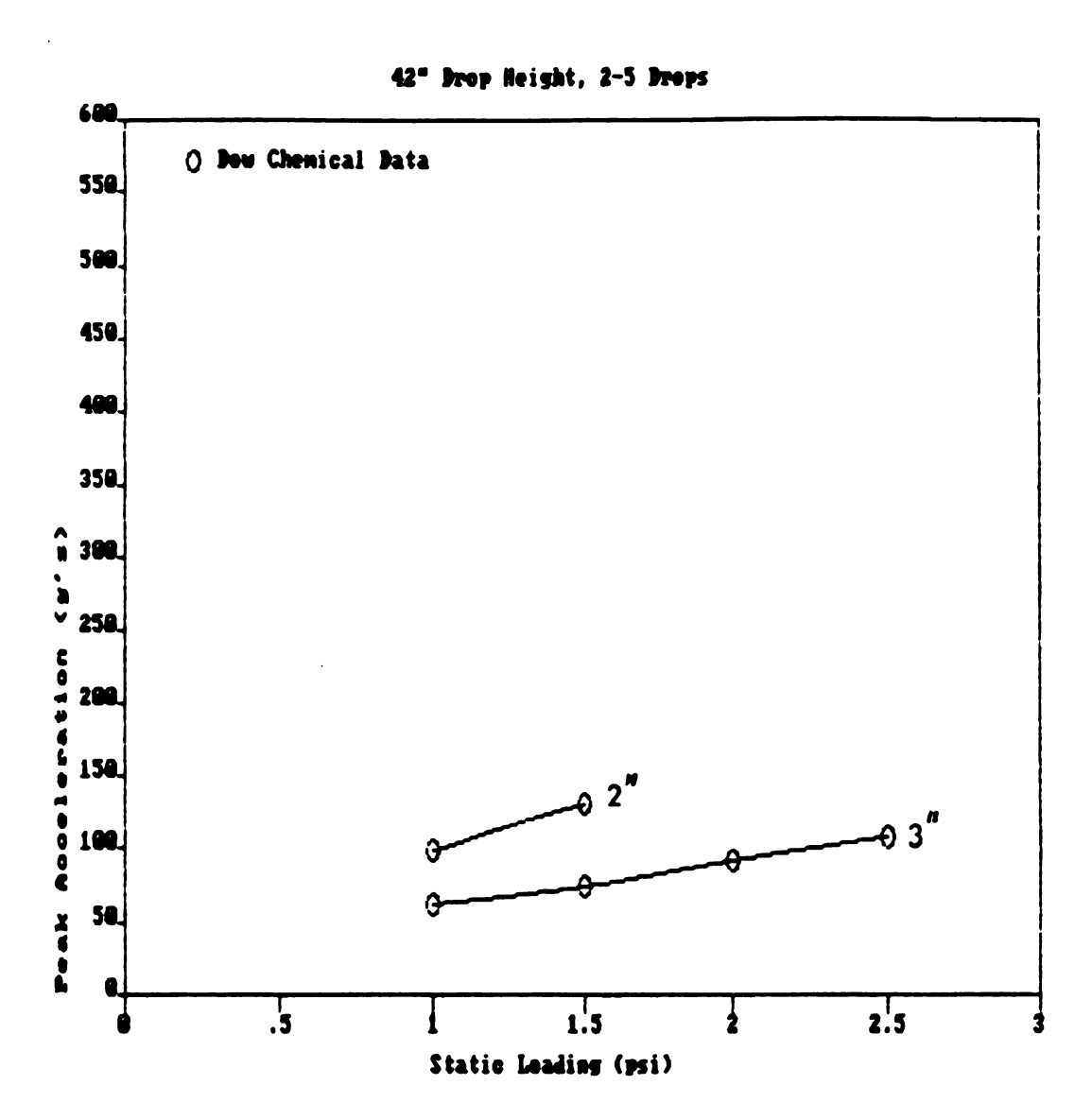


Figure 18. Dow Chemical Co. data for a 42" drop height

An additional benefit derived from using the high-speed video method is that the maximum cushion strain can be readily determined upon playback of the recording. In comparison, peak compression values are difficult to obtain, if not impossible, using the accelerometer method. The percent compressions during peak cushion deformation are calculated in Table 4 and shown in Figure 19. Note the extreme degree of cushion compression that occurs. Since the sides of the cushions were not observed to bulge appreciably during this compression, it follows that the volume of the cushion decreases dramatically. When this occurs, it is natural to assume that the density, and therefore the shock-pulse frequency experienced during the impact, increases dramatically.

Table 4. Percent total compression at peak cushion deformation for 2" and 3" thick cushions

		h:	=30	h:	= 36 "	h=42"		
S-L,	sample	T=2"	T=3"	T=2"	T=3"	T=2"	t=3"	
1.0	A	82%	69%	89%	77%	91%	80%	
1.0	В	83%	68%	90%	79%	92%	81%	
1.5	A	92%	79%	99%	92%	99%	95%	
1.5	В	95%	79%	97%	92%	99%	94%	
2.0	A	96%	90%	99%	94%	99%	96%	
2.0	В	98%	90%	99%	93%	99%	95%	
2.5	A	99%	95%	99%	97%	99%	99%	
2.5	В	99%	94%	99%	97%	99%	99%	
				•		1		

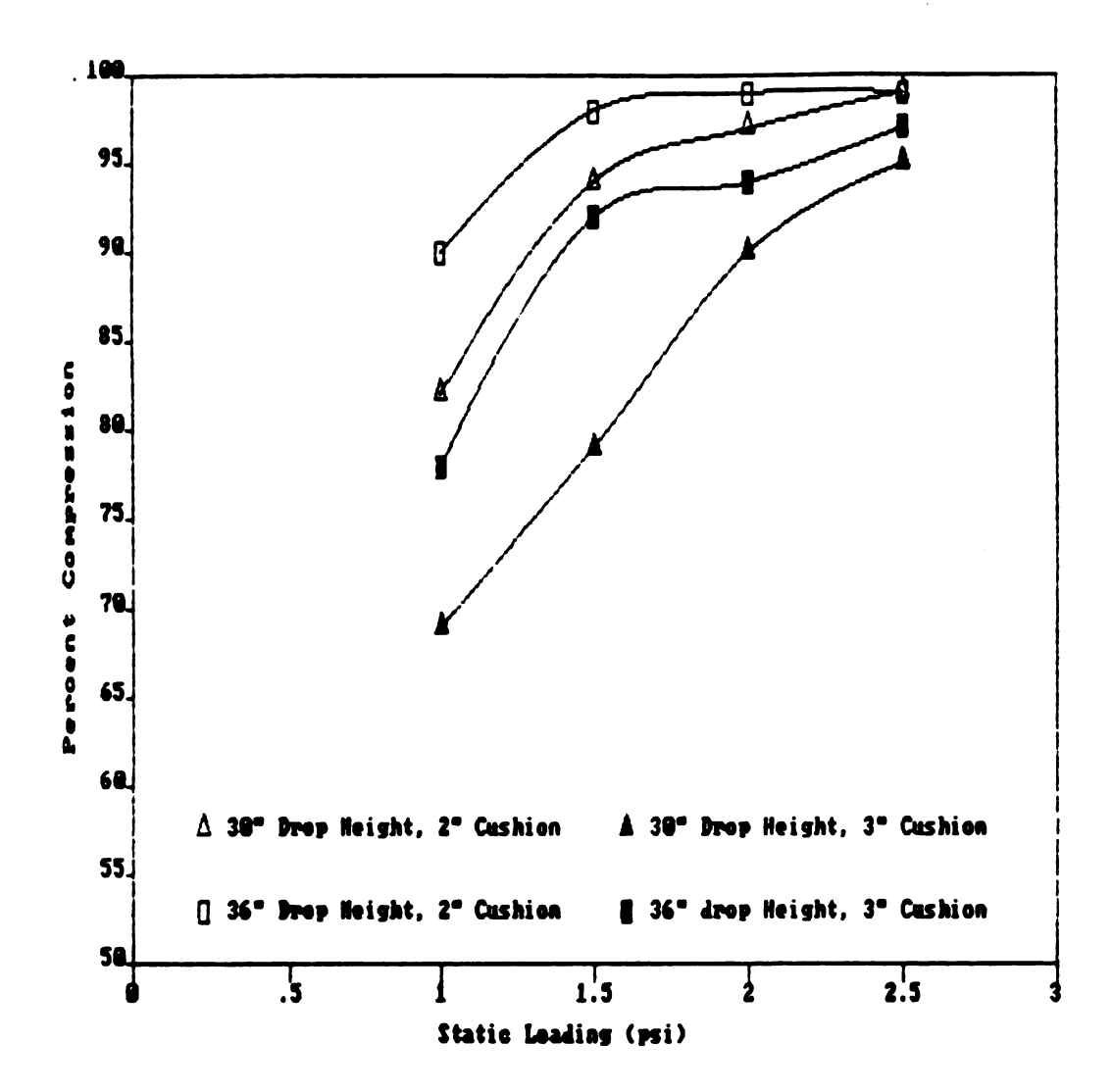


Figure 19. Percent compression at peak cushion displacement

CHAPTER 4

LIMITATIONS AND SUGGESTIONS FOR FUTURE RESEARCH

When comparing the results obtained using the highspeed video method with the results obtained using the
accelerometer method, it is clear that they may differ
by as much as 100%. Only part of this discrepancy may
be attributed to the high-speed video method. The
remainder must be associated with the accelerometer
method. Some obvious problems encountered during the
drop tests using the high-speed video method that were
not covered previously are covered below.

The contrast between the white cushion material and the moving test platen tended to decrease the most at peak displacement and this may have increased reading errors somewhat. Blurring or wash-out of certain "key" frames also resulted in greater reading errors. Ambiguous portions were double-checked in an attempt to reduce these errors.

Possible improvements include improving the contrast between the test platen and the cushion material, and using a faster camera speed (not currently possible on the camera used) with a greater resolution.

The contrast could also be improved by using the proper combination of surface characteristics. Both black-and-white paper, and black paper and aluminum foil were tried as platen coverings. The best results were obtained with the black-and-white paper. It is possible that other surface coverings may work better. This would have helped to positively locate the pixel corresponding to maximum cushion compression.

A faster camera speed would result in a smoother image on the video screen. Often the platen edge would "jump" 5 pixels or more in 1 "frame". While this occured to a lesser extent at the critical moment of peak cushion deformation, it must still be assumed that reading errors occurred whenever the platen edge was blurred over a span of many pixels. A faster camera speed would also allow for greater resolution through "zooming-in" at the critical moment of peak cushion displacement. assumes some prior knowledge of the approximate value of this peak compression however. Since a greater number of pixels would cover the smaller critical area. finer measurements could be made. This would in require a greater camera speed in order to maintain a reasonably smooth record.

The number of replications was limited by the availability of film for the Kodak video system. A test project using a greater number of replications may give better results but would require more film.

While the above arguments point to the high-speed video method as being responsible for the difference between the two methods, it is entirely likely that the accelerometer method is equally responsible for the discrepency. The accelerometer method has an accuracy of $\pm 14\%$ (See Appendix B) which accounts for at least part of the difference.

The data shows a tendency towards greater disparity at higher static loadings with greater drop heights. See Figures 13 through 15. These impacts produce very cushion strains (from 90% - 99%). In these high density the cushion increases instances. the of dramatically (from 10 to 100 times in a very short time) which in turn raises the cushion stiffness and high q values. The accelerometer must leads to therefore be capable of responding to large changes in acceleration over small time periods and may not be able to do so depending on its natural frequency. The accelerometer may also be producing exaggerated data as

the result of shock amplification (10). This may also help explain the variation in g's measured between the accelerometer results and the cushion curves for Ethafoam 220 provided by Dow Chemical. It does not however completely explain the variation between the high-speed video method and the other results. Further testing needs in order to more fully understand the errors inherent in each method.

CHAPTER 5

CONCLUSION OF RESULTS

The high-speed video method is a useful alternative for for determining peak acceleration during cushioned impacts. While there are problems associated with this method, few affect the accuracy of the results. Furthermore these problems, outlined in Chapter 2, may be expected to decline as the technology of high-speed video becomes more prevalent. The high-speed video method also is capable of several functions not currently possible using the accelerometer method.

Since a time record is made of the entire compression-expansion cycle, peak displacement is very easy to obtain. This study shows that cushions deform much more upon impact than previously thought. This is shown in Figure 19. In addition, since there is no contact with the test sample, it is possible to record the dynamics of cushioned drops on extremely lightweight samples. One possible example would be to measure the dynamic characteristics of thin films without having to deal with the weight of an accelerometer. Any analysis situation where the weight of the accelerometer is a concern is a possible candidate for the high-speed video method.

APPENDIX A:

Experimental Data

Table 5. Position of Platen vs. Time for 2" cushions

h / T / S		Cshn Top		-6	-3	l Peak	+1	+6		Cshn Btm
30"/ 2"/ 1	.0 psi	93	66 66	46 45	30 30	23	29 26	41 38	56 52	8 8
30"/ 2"/ 1	.5 psi	92	68 62	47 40	27 21	15	21 21	34 36	50 52	1 8 1 8
30"/ 2"/ 2	2.0 psi	92	69 69	47 47	27 27	11	18 18	33 32	49 48	1 8 1 9
30"/ 2"/ 2	2.5 psi	91	68 66	45 43	24 23	9 1	19 20	34 36	50 52	1 8
36"/ 2"/ 1	.0 psi	94	71 74	4 6 50	27 29	18	26 24	4 2 4 0	60 57	1 9
36"/ 2"/ 1	.5 psi	89 i 89 i	76 71	51 45	27 23	111	23 26	41 43	60 62	110
36"/ 2"/ 2	2.0 psi	93 i 91 i	74 75	49 49	26 26	9 1	21 22	39 40	58 58	, 1 9 1 9
36"/ 2"/ 2	2.5 psi	90	76 74	53 49	28 25	7	22 24	38 41	56 60	1 6
42"/ 2"/ 1	.0 psi	86	70 69	47 44	25 22	13	20 22	35 39	53 57	1 6 1 6
42"/ 2"/ 1	.5 psi	81 i 79 i	73 69	47 42	23 19	. 3 i	15 17	33 35	49 54	1 3
42"/ 2"/ 2	2.0 psi	82 i 81 i	75 70	48 44	25 20	8 1	20 23	38 41	57 61	! ! 8 ! 8
42"/ 2"/ 2			102	76 73	51 47	1 31 1 1 31 1	45 47	64 64	81 81	132
111						T1				T

all measurements in pixels.

h = equivalent drop height in inches
T = cushion thickness in inches

S-L = cushion static loading in p.s.i.

Table 6. Position of platen vs. time for 3" cushions

h /	т /	S-L		Cshn I		-6	-3	l Peak	+3	+6		Cshn Btm
30"/	2"/	1.0	psi	118		50 54	43 46	41	44	50 53		1~10
30"/	2"/	1.5	psi	1 1181 1 1151	57	46 44	36 33	33	35 34	42 42		~12 !~11
30"/	2"/	2.0	psi		52	37 37	27 27	24	28 29	37 39	48 51	1 14
30"/	2"/	2.5	psi	113		37 32	24 22	20	25 28	35 39	48 52	1 15
36"/	2"/	1.0	psi	117		50 46	37 34	33	38	48 48	62 63	1 8
36"/	2"/	1.5	psi	116		42 43	25 26	17	24	37 35	52 50	! 8 ! 8
36"/	2"/	2.0	psi	114		42 38	24 21	14	21	34 37	50 53	! 8 ! 8
36"/	2"/	2.5	psi	114		41 41	22 22	11	19	33 34	50 50	1 8
42"/	2"/	1.0	psi	121		49 48	35 34	29	34	45 46	60 61	1 6
42"/	2"/	1.5	psi	116		42 44	22 24	11	18	33 32	51 50	1 5 1 4
42"/	2"/	2.0	psi	112		40 45	18 23	1 8 1 1 9 1	17	33 32	52 49	1 4
42"/	2"/	2.5	psi	114		45 44	23 22	1 8 I	17	34 35	53 54	1 1 8 1 9
								•	•			•

all measurements in pixels

h = equivalent drop height in inches
T = cushion thickness in inches

S-L = cushion static loading in p.s.i.

Table 7. Data for accelerometer method, 2" cushions

95 g 76 g
143 g 140 g
175 g 178 g
255 g 260 g
105 g 113 g
280 g 275 g
310 g 325 g
460 g 460 g
140 g 158 g
350 q 345 q
430 g 430 g
590 g 570 g

h = equivalent drop height in inches
T = cushion thickness in inches

S-L = cushion static loading in p.s.i.

Table 8. Data for accelerometer method, 3" cushion

h / T / S-		lliscope tting	Height	Acceleromtr Sensitivity	
30"/ 2"/ 1.0		mv/div mv/div		2.0 mv/g 2.0 mv/g	1 36 g 1 35 g
30"/ 2"/ 1.9		mv/div mv/div	4.7 divi	2.0 mv/g 2.0 mv/g	i 47 g i 44 g
30"/ 2"/ 2.0		mv/div mv/div		2.0 mv/g 2.0 mv/g	1 63 g 1 65 g
30"/ 2"/ 2.9		mv/div mv/div		2.0 mv/g 2.0 mv/g	1103 g 1 93 g
36"/ 2"/ 1.0		mv/div mv/div	2.0 divi 5.4 divi	2.0 mv/q 2.0 mv/g	1 50 q 1 54 q
36"/ 2"/ 1.9		mv/div mv/div	3.7 divi 3.6 divi	2.0 mv/g 2.0 mv/g	93 g 1 90 g
36"/ 2"/ 2.0	•	mv/div mv/div	4.7 divi		1118 g 1110 g
36"/ 2"/ 2.9		mv/div mv/div		2.0 mv/g 2.0 mv/g	1158 g 1163 g
42"/ 2"/ 1.0		mv/div mv/div	5.7 divi 6.3 divi	2.0 mv/g 2.0 mv/g	1 57 g 1 63 g
42"/ 2"/ 1.9		mv/div mv/div	5.0 divi	2.0 mv/g 2.0 mv/q	1125 g 1135 g
42"/ 2"/ 2.0		mv/div mv/div	3.2 divi 6.7 divi	2.0 mv/q 2.0 mv/g	1160 q 1168 q
42"/ 2"/ 2.5	5 psil 100 100		4.9 divi	2.0 mv/g 2.0 mv/q	1245 g 1235 g +

h = equivalent drop height in inches
T = cushion thickness in inches

⁼ cushion thickness in inches

S-L = cushion static loading in p.s.i.

Appendix B Measurement Errors

The errors associated with this study may be divided into accelerometer method errors, drop tester errors, and video method errors.

Accelerometer method errors:

Accelerometer: ±2%

Coupler: ±5%

Oscilloscope: ±3%

Reading error: ±4%

Sensitivity error: unknown

(See Appendix C)

Total Error : ±14%

Drop tester height errors:

Drop height error: ±2%

Total Error : ±2%

Video method errors:

An obvious technique error resulting in the blurring of some of the recorded video images is known to have occurred. When this occurred, the exact position of the platen edge was not easily determined. The range of uncertainty was at most 1 pixel. To maximize the effect of this uncertainty on the instantaneous acceleration [eq.15], the displacements y_1 , y_3 , y_5 , and y_7 should be increased by 1 pixel, and the displacements y_2 , y_4 , and y_6 should be decreased by 1 pixel. This is illustrated in Figure 20. Likewise, to minimize the instantaneous acceleration, the displacements

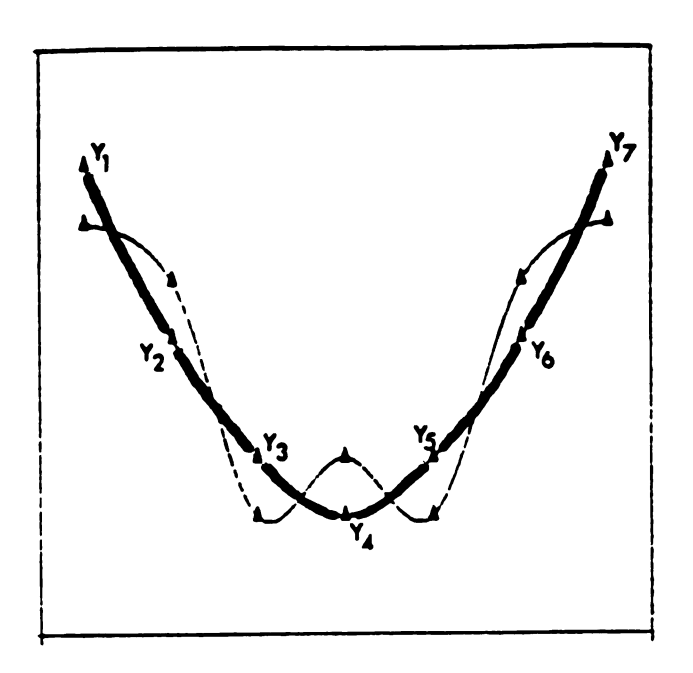


Figure 20. Video error analysis, maximum case

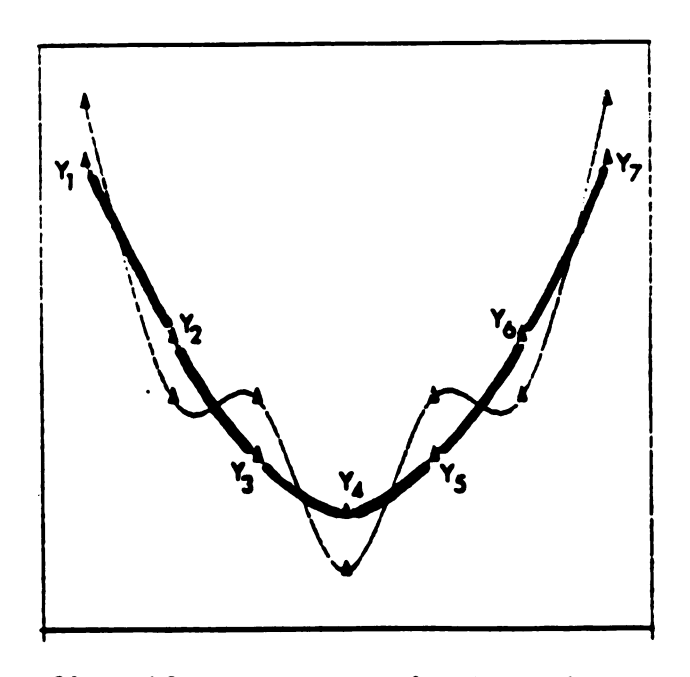


Figure 21. Video error analysis, minimum case

 y_1 , y_3 , y_5 , and y_7 should be decreased by 1 pixel and displacements y_2 , y_4 , and y_6 should be increased by 1 pixel. This is shown in Figure 21. Since the maximum and minimum accelerations obtained in this way represent the two extremes (assuming no more than a ± 1 pixel error) the actual acceleration is expected to be somewhere in between them. The average error for the acceleration associated with this range of values using the test data is $\pm 25\%$. A more accurate assessment of the position error is .5 pixels, which would reduce the error to $\pm 12.5\%$.

Another source of error the changing camera angle. See Figure 6. This error is greatest at peak displacement if the camera is initially focused on the top of the cushion (as in these tests). By focusing on the cushion bottom, this error would have been less. This error was estimated to be $\pm 2\%$ for a typical drop.

Total Error: ±27%

Appendix C Finite Difference Analysis

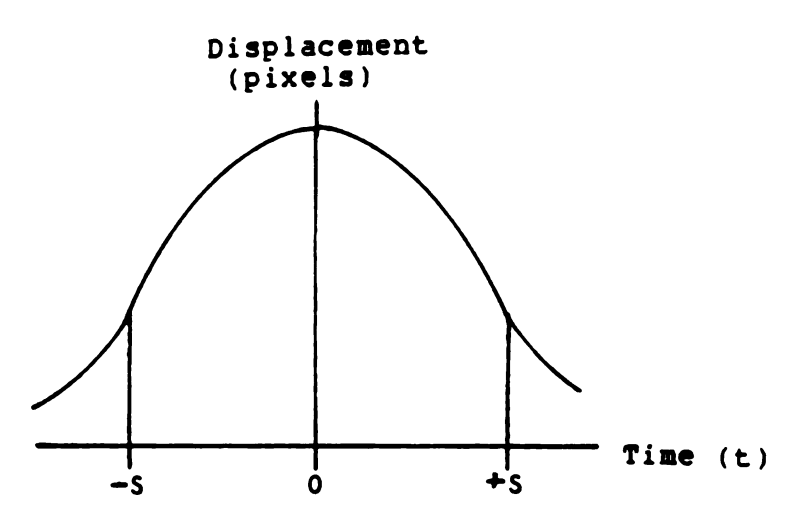


Figure 22. Typical 3-point data spread

A quadratic spline can be fitted to these points by
forcing the displacement vs. Time equation,

$$Y = a + b(t) + c(t)^2$$
 [Eq. 4]

to fit the data, which requires that:

When:
$$t = -s$$
, $Y = a - b(s) + c(s)^2$ [Eq. 5]

When:
$$t = 0$$
 $Y = a + b(0) + c(0) = a$ [Eq.6]

When:
$$t = +s$$
 $Y = a + b(s) + c(s)^2$ [Eq. 7]

The solution of this system of equations for c gives:

The values of a and b are not needed as the acceleration is the second derivitive of Eq.4 with respect to time and this involves only c;

$$Y = a + b(t) + c(t)$$
 [Eq.4]
 $Y' = 0 + b(1) + 2c(t)$
 $Y'' = 0 + 0 + 2c = \frac{y - 2y + y}{(s^2)}$ [Eq.9]

The value of y" in Eq.9 is the peak deceleration associated with the 3-point finite difference approximation to the true acceleration.

An improved finite difference expression for the acceleration uses a 5-point data spread as illustrated in Figure 23.

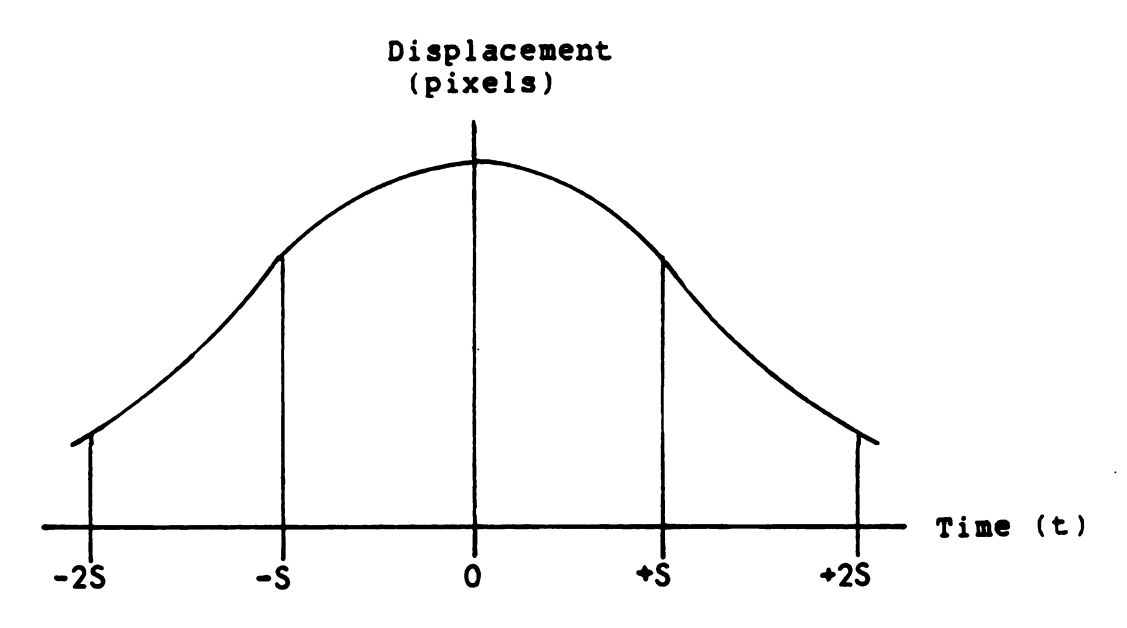


Figure 23. Typical 5-point data spread

The spline to be fitted to this data is a quadratic polynomial,

$$Y = a + b(t) + c(t^2) + d(t^3) + e(t^4)$$
 [Eq.10]

$$Y'' = 0 + 0 + 2c + 6d(t) + 12e(t^2)$$
 [Eq.11]

Eq. 11 is the instantaneous acceleration at any given moment in time, (t). At t=0 where the deceleration is desired, the result is seen to be dependent again only on c:

$$Y'' = 2c \qquad [Eq.12]$$

The solution to the system of equations obtained by forcing the spline in Eq.10 to fit the displacement y at the five sampling times in Figure 23 gives;

$$c = \frac{-y + 16y - 30y + 16y - y}{24(s^2)}$$
 (Eq.13)

Therefore, by substituting Eq.13 into Eq.12:

$$g = Y'' = \frac{-y + 16y - 30y + 16y - y}{12(s^2)}$$
 [Eq.14]

Fitting a 7-point data spread as in Figure 24 to a 6th order polynomial gives an even better finite difference approximation to the true acceleration,

$$g = \frac{2(y_1)-27(y_2)+270(y_3)-490(y_4)+270(y_5)-27(y_6)+2(y_7)}{180(s^2)}$$

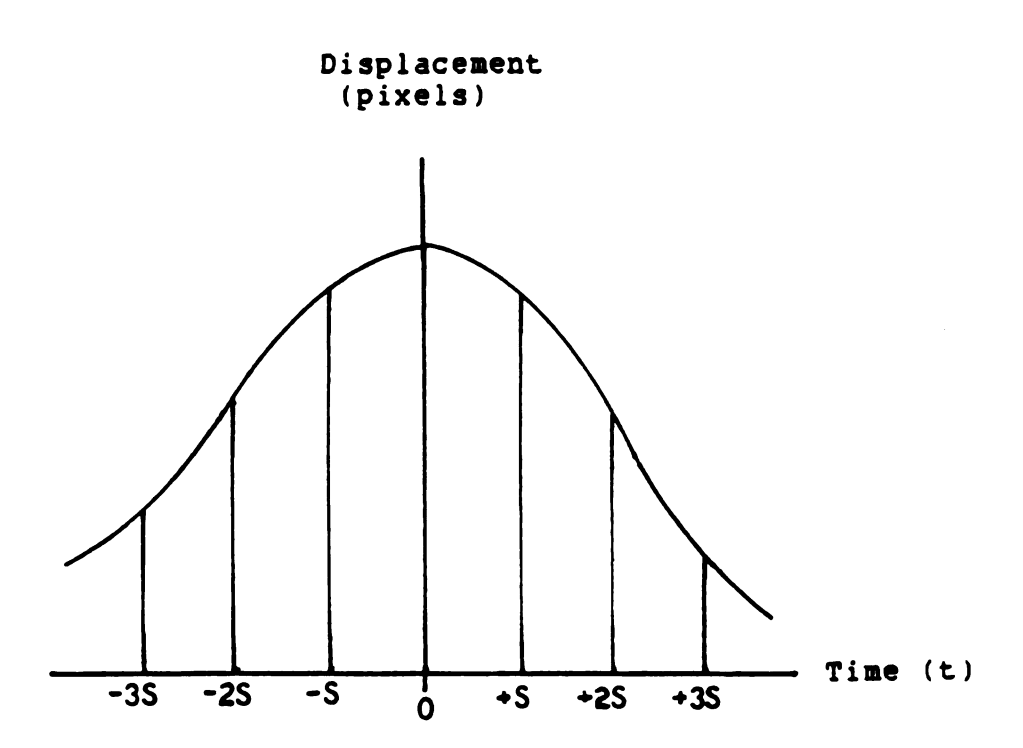


Figure 24. Typical 7-point data spread

APPENDIX D EQUIPMENT SPECIFICATIONS

Cushion Test Machine: Lansmont model 23 cushion tester

Machine Type Free-fall

9" x 9" Platen Size

12.8 lbs. Platen Weight

Ballast Kits $1 \times 6.4 lbs.$ 1 x 12.8 lbs.

2 x 25.6 lbs. 2×32.0 lbs.

Controls 24 vdc control

system (standard)

Table Lifting/Positioning By electric hoist

Maximum Equivalent Free-45 inches

Fall Drop Height

Power Requirements 115 vac, 60 hz,

8 amps.

Pneumatic Requirements Air or nitrogen at

80 - 120 p.s.i.

Accelerometer: PCB model 305 A05 piezoelectric

Resonant Frequency 40 khz

Reference Voltage Sensitivity 2.00 mv/g @100 hz

Note: Although this value was used for this study, it must be assumed that an error due to the frequency response characteristics of the accelerometer was present. For best results, the accelerometer used should be calibrated over the entire range of

shock frequencies expected.

1000 q's Range

Coupler: Kistler model 5116

Frequency Response 5% from .5 hz to

250 khz

Input/Output Coupling Input is AC

coupled to output buffer amplifier.

Full Scale Signal 20 v p-p

Impedance 20 ohms

Noise .18 mv rms

Power Source 110 vac, 60 hz,

10 mA

Oscilloscope: Kikusui model D55 6520

Screen Type Direct viewing, bi-stable storage

tube.

Acceleration Voltage Appx. 3.15 Kv

Writing Speed 25 div/msec

Vertical Sensitivity 5 mv at 5v/div

Frequency Bandwidth DC - 20 mhz, -3 dB

Rise Time 17 nsec

Input Impedance l Mega-Ohm

Maximum Allowable Input 400 v

Voltage

High-Speed Video Camera: Kodak Ectapro 1000

Imager Resolution 192 x 240 pixels

Imager Lens Mount C-mount

Tripod Mount 1/4-20 and 3/8-16

standard ANSI

Recording Technique Linear FM

Recording Medium 1/2" high-density

magnetic tape

Tape Handling Cassette (700 ft)

Recording Rates 30,60,125,250,500,

1000 frames/sec

Recording Time From 30 seconds to

16 minutes based

on speed used

Playback Continuous, jog,

or single step

Video Output NTSC and PAL

Power Requirements 110 vac, 60 hz,

8 amps

LIST OF REFERENCES

- 1. ASTM D-3332, Mechanical-Shock Fragility of Products, using Shock Machines, 1983.
- James W. Goff and Diana Twede, <u>Shake and Break:</u>
 <u>Laboratory Adventures in Shock and Dynamics</u>,
 (Michigan State University, School of Packaging)
 1983, pp. 11-17.
- 3. James W. Goff, <u>Control of Damage in Shipment: The Development of a Telemetry Shock Measuring System</u>, Technical Report No. 14, (Michigan State University, School of Packaging), 1968
- 4. Richard K. Brandenburg and Julian Lee, <u>Fundamentals</u>
 of <u>Packaging Dynamics</u>, 2nd Ed. Minneapolis, MTS
 Systems Corporation, 1985.
- 5. Gary Burgess, "Some Thermodynamic Observations on the Mechanical Properties of Cushions," <u>Journal of Cellular Plastics</u>, 1987.
- 6. Cyril Harris and Charles Creed, <u>Shock and Vibration</u>
 <u>Handbook</u>, 2nd Ed. McGraw-Hill Book Company, 1976.
- 7. Brandenburg and Lee, <u>Fundamentals of Packaging</u>
 Dynamics, pg.115
- 8. ASTM D-1596 Shock Absorbing Characteristics of Package Cushioning Materials, 1983.
- 9. Harris and Creed, <u>Shock and Vibration Handbook</u>, pp. 12.1-12.5
- 10. Brandenburg and Lee, <u>Fundamentals of Packaging</u>
 Dynamics. pp. 86-93.

HICHIGAN STATE UNIV. LIBRARIES
31293005712181